Kongju National University
Department of Physics Education

A Crash Course in Quantum Transport II: Various Mesoscopic Interactions

Kongju National University
Dept. of Physics Education

Sang-Jun Choi

Summer School of Mesoscopic Physics
@PKNU, 2025. 5. 24

What is Mesoscopic Quantum Transport

- **Mesoscopic quantum transport?**
- **Why 'transport?'**

→ Transport reveals information of transported objects

→ Imagine we are in a dark room!

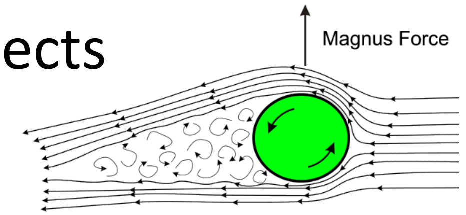

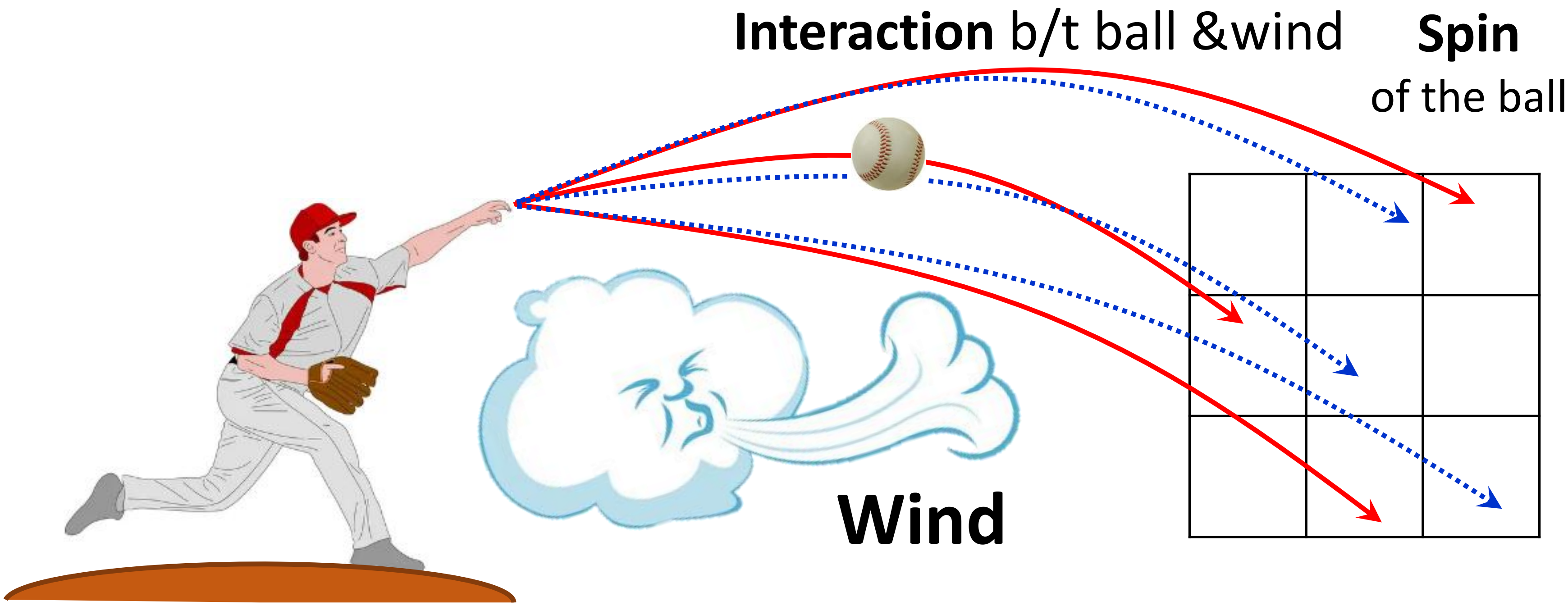

Figures from depositphotos.com

What is Mesoscopic Quantum Transport

- **Mesoscopic quantum transport**?
- **Why 'transport'**: Transport reveals information of transported objects
- **Which one is 'quantum'**: ptls are superposed, interfered, or entangled

  → New phenomena with the same game setting?

  = New quantum particle!

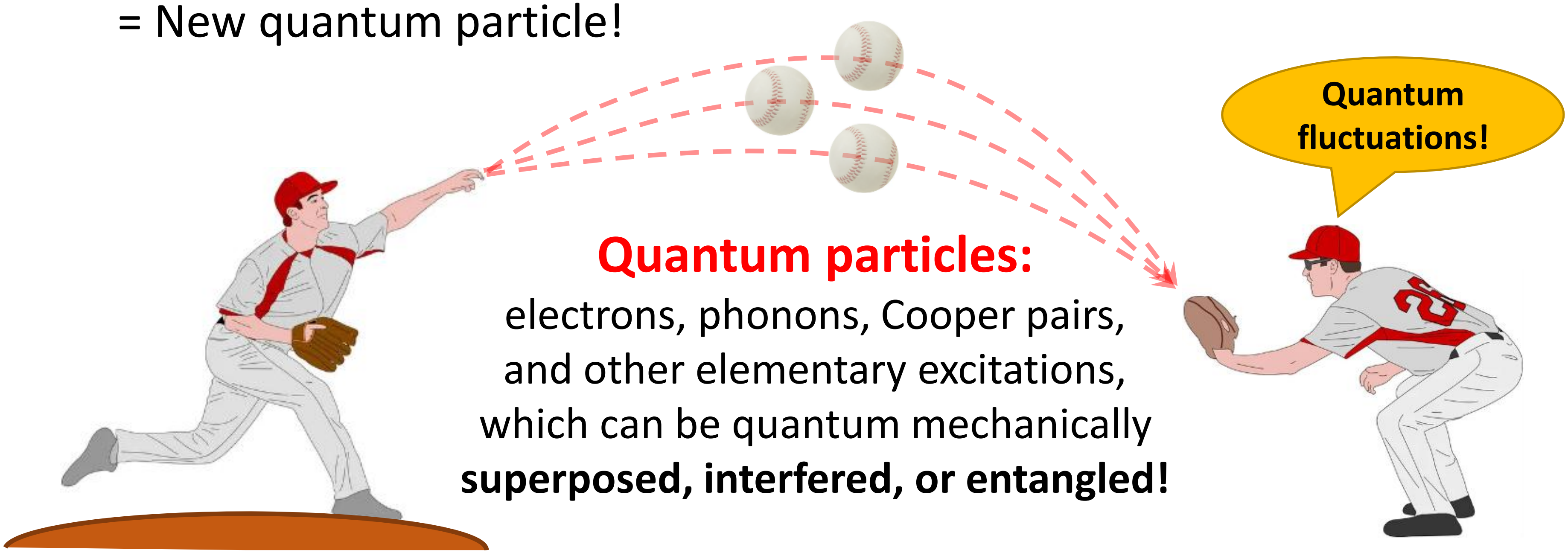

Quantum particles:
electrons, phonons, Cooper pairs,
and other elementary excitations,
which can be quantum mechanically
superposed, interfered, or entangled!

Figures from depositphotos.com

What is Mesoscopic Quantum Transport

- **Mesoscopic quantum transport**?
- **Why 'transport'**: Transport reveals information of transported objects
- **Which one is 'quantum'**: ptls are superposed, interfered, or entangled
- **What's meso-scopic systems**

  → **Playground** for **quantum** baseballs (not too large: macro-scopic)

  but **well-controllable & designable** (not too small: micro-scopic)

Competition b/t **various scales matter**!

We can place **quantum** pitchers, catchers, fans on the field, **as we want!**

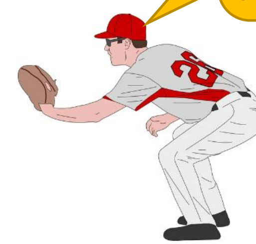

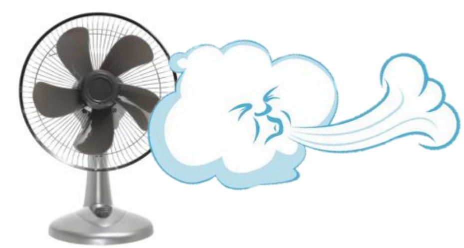

Physics of MQT: perfect conductor

- **Perfect conductor**

we assume: size of conductor, $L << L_m$, L_φ. But $\lambda_F < W$ w/ subbands

Reflectionless contacts (no backscattering at contact)

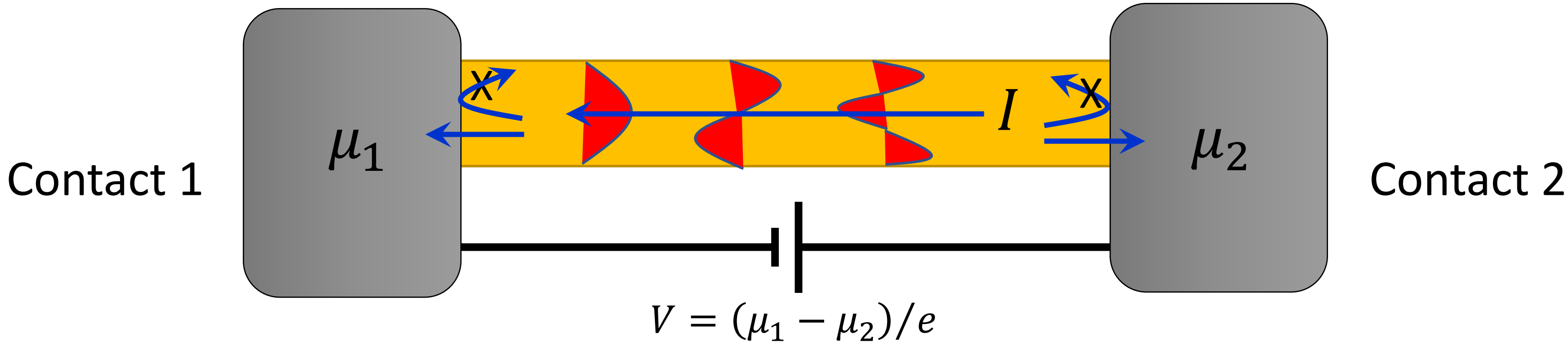

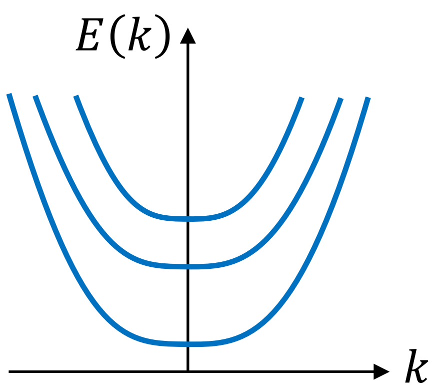

PRL **62**, 300 (1989)

Physics of MQT: perfect conductor

- **Perfect conductor**

  we assume: size of conductor, $L << L_m, L_\varphi$. But $\lambda_F < W$ w/ subbands

  Reflectionless contacts (no backscattering at contact)

- **Calculating the current**

(zero temp.) $$I^+ = \frac{2e}{h} M\mu_1 \ \& \ I^- = -\frac{2e}{h} M\mu_2$$

Opposite sign due to opposite group velocity

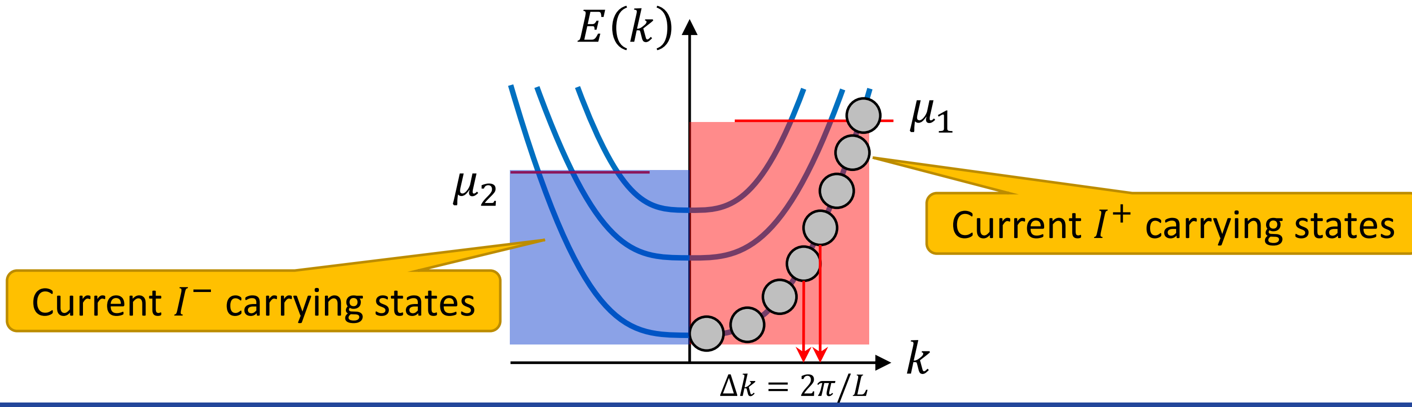

Physics of MQT: perfect conductor

- **Perfect conductor**

we assume: size of conductor, $L \ll L_m$, L_φ. But $\lambda_F < W$ w/ subbands

Reflectionless contacts (no backscattering at contact)

- **Calculating the current**

(zero temp.) $$I^+ = \frac{2e}{h} M\mu_1 \;\;\&\;\; I^- = -\frac{2e}{h} M\mu_2$$

$$I = I^+ + I^- = \frac{2e}{h} M(\mu_1 - \mu_2) = \frac{2e^2}{h} M \frac{\mu_1 - \mu_2}{e} = \frac{2e^2}{h} MV$$

G of a perfect conductor = integer multiple of conductance quantum

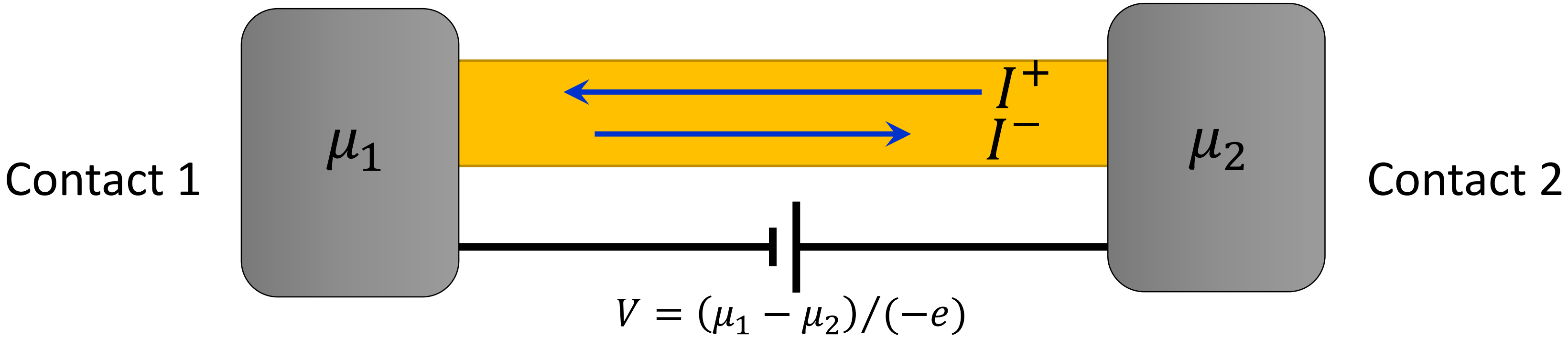

Physics of MQT: perfect conductor

- **Perfect conductor**

  we assume: size of conductor, $L << L_m$, L_φ. But $\lambda_F < W$ w/ subbands

  Reflectionless contacts (no backscattering at contact)

- **Quantized conductance**

$$G = \frac{2e^2}{h} M$$

Contact resistance

$$R_c = \frac{h}{2e^2 M} = \frac{12.9}{M} \text{ k}\Omega$$

- **Where is the voltage drop?**

  Ans. at the contacts

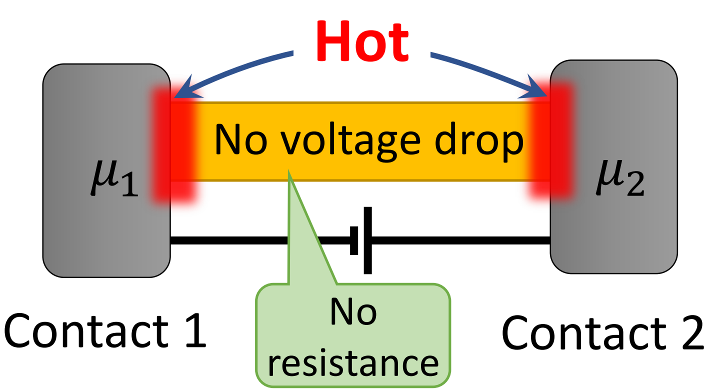

Energy dissipation should occur to fit into B.C. at infinity

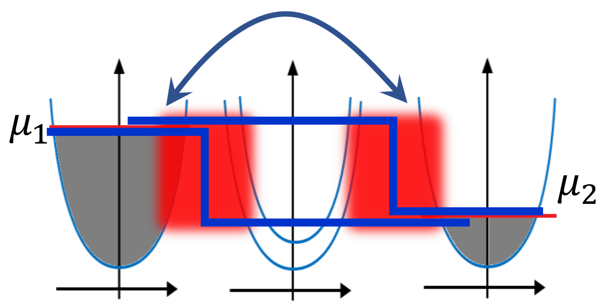

i) Translational symmetry is broken at contacts
ii) Contacts are irremovable

No matter how we define the voltage drop, it occurs **at the contacts**

Physics of MQT: perfect conductor

- **Perfect conductor**

  we assume: size of conductor, $L << L_m, L_\varphi$. But $\lambda_F < W$ w/ subbands

  Reflectionless contacts (no backscattering at contact)

- **Persistent Current & Scales**

How long the time should be to be 'persistent?'

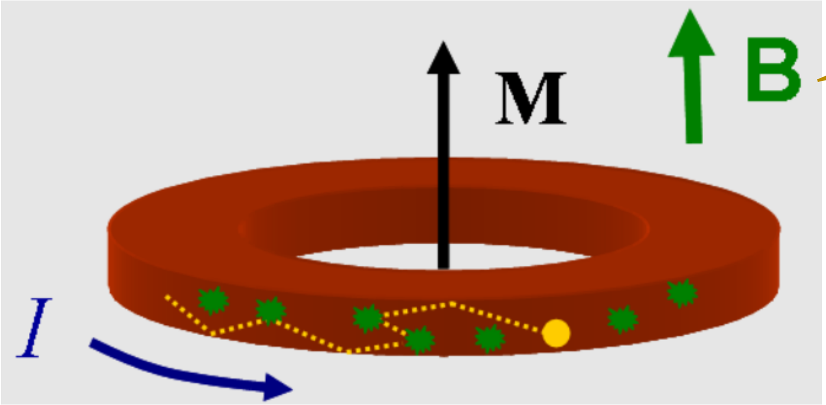

M. Büttiker, Y. Imry, R. Landauer, *Josephson behavior in small normal one-dimensional rings*, Phys. Lett. A. **96**, 365 (1983)

Measuring elusive "persistent current" that flows forever, R&D Daily. October 12, (2009)

Physics of MQT: Not perfect but ballistic conductor

- **Ballistic conductor w/ a single impurity:** size of conductor, $L < L_\mathrm{m}$

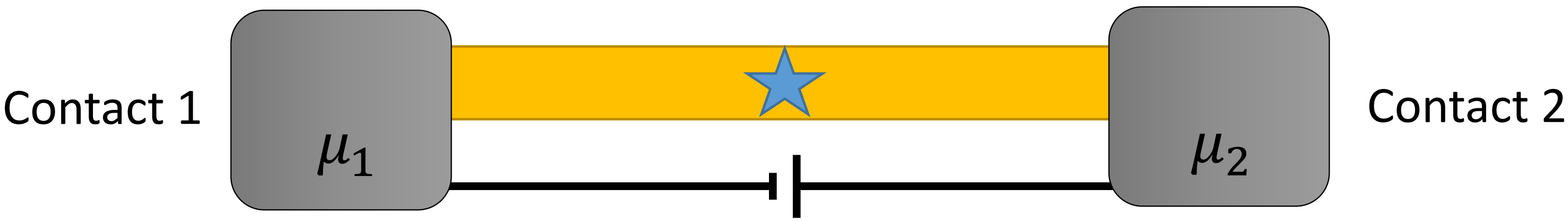

- **Scattering Matrix**

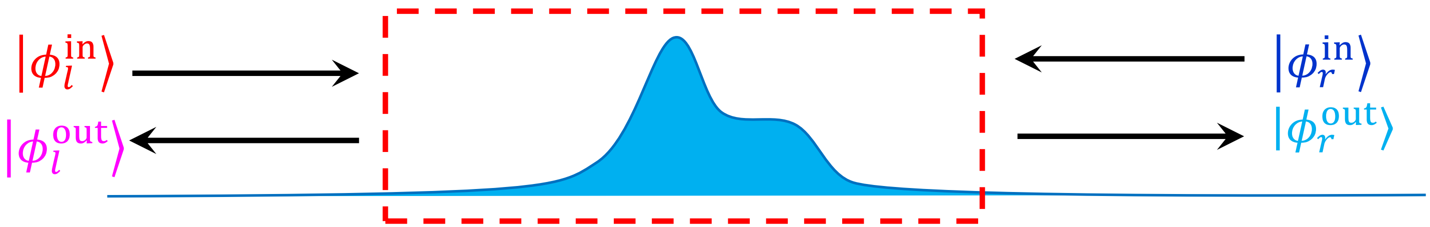

$|\phi_l\rangle \equiv \lim_{x\to-\infty}|\psi\rangle$

$|\phi_r\rangle \equiv \lim_{x\to\infty}|\psi\rangle$

General solution $\hat{H}|\psi\rangle = E|\psi\rangle$: $|\phi_l\rangle = A|\phi_l^{\mathrm{i}}\rangle + B|\phi_l^{\mathrm{o}}\rangle$ & $|\phi_r\rangle = C|\phi_r^{\mathrm{o}}\rangle + D|\phi_r^{\mathrm{i}}\rangle$.

Undergraduate courses, we deal with two cases: (i) left & (ii) right incidence. We know

(i) $B = rA$ & $C = tA$ & $D = 0$: $\quad |\phi_l\rangle = A|\phi_l^{\mathrm{i}}\rangle + rA|\phi_l^{\mathrm{o}}\rangle$ & $|\phi_r\rangle = tA|\phi_l^{\mathrm{o}}\rangle$

(ii) $B = t'D$ & $C = r'D$ & $A = 0$: $+\,\big]\; |\phi_l\rangle = t'D|\phi_l^{\mathrm{o}}\rangle$ & $|\phi_r\rangle = r'D|\phi_r^{\mathrm{o}}\rangle + D|\phi_r^{\mathrm{i}}\rangle$.

General solution is

$$|\phi_l\rangle = A|\phi_l^{\mathrm{i}}\rangle + (rA + t'D)|\phi_l^{\mathrm{o}}\rangle \ \& \ |\phi_r\rangle = (tA + r'D)|\phi_r^{\mathrm{o}}\rangle + D|\phi_r^{\mathrm{i}}\rangle.$$

Physics of MQT: Not perfect but ballistic conductor

- **Ballistic conductor w/ a single impurity:** size of conductor, $L < L_{\mathrm{m}}$

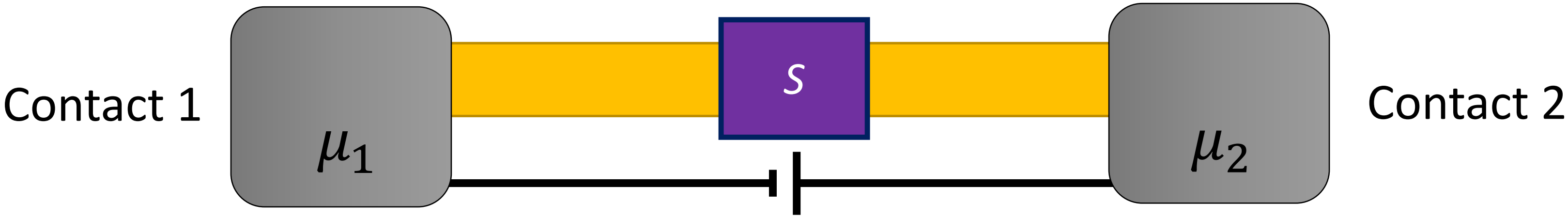

- **Scattering Matrix**

$|\phi_l^{\mathrm{i,o}}\rangle \equiv \lim_{x\to-\infty} |\psi^{\mathrm{i,o}}\rangle$

$|\phi_r^{\mathrm{i,o}}\rangle \equiv \lim_{x\to\infty} |\psi^{\mathrm{i,o}}\rangle$

General solution: $|\phi_l\rangle = A|\phi_l^{\mathrm{i}}\rangle + (rA + t'D)|\phi_l^{\mathrm{o}}\rangle$ & $|\phi_r\rangle = (tA + r'D)|\phi_r^{\mathrm{o}}\rangle + D|\phi_r^{\mathrm{i}}\rangle$.

$$\begin{pmatrix} B \\ C \end{pmatrix} = \begin{pmatrix} r & t' \\ t & r' \end{pmatrix} \begin{pmatrix} A \\ D \end{pmatrix} = S \begin{pmatrix} A \\ D \end{pmatrix}$$

If interested only in amplitudes of scattering states at infinity, only thing we need to know is

Physics of MQT: Not perfect but ballistic conductor

- **Ballistic conductor w/ a single impurity:** size of conductor, $L < L_m$

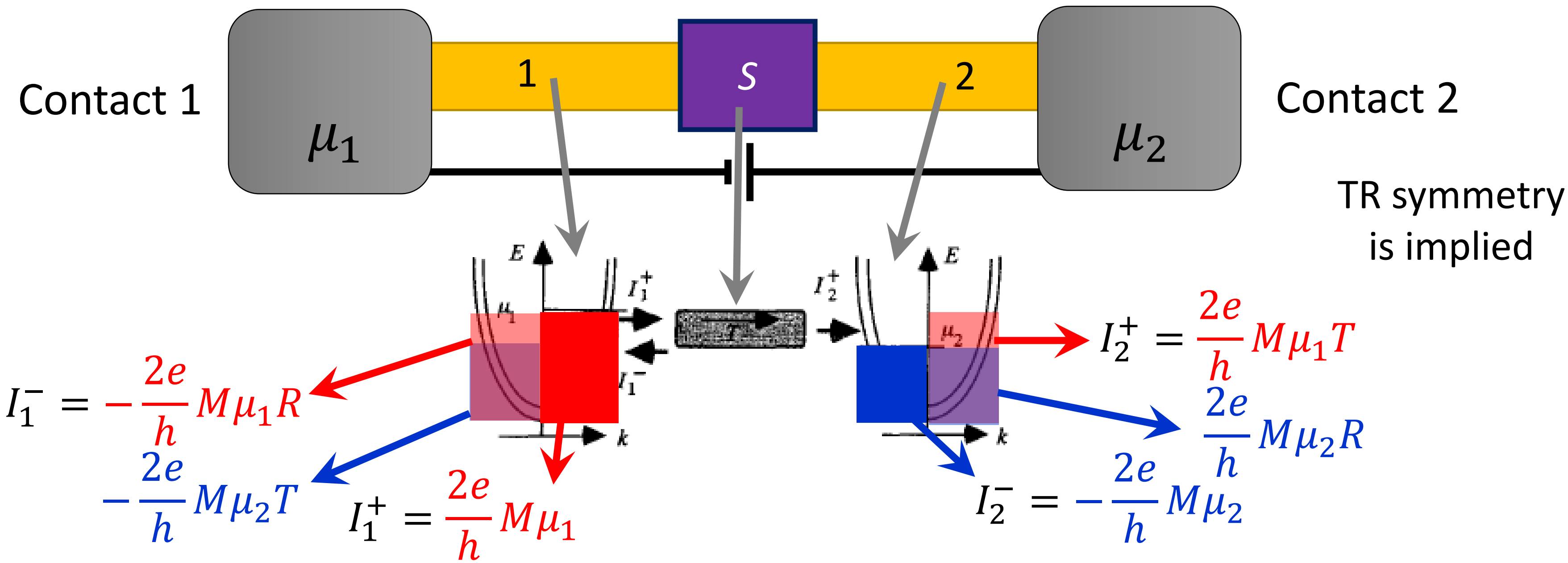

Total current at lead 1:

$$I_1 = I_1^+ + I_1^- = \frac{2e}{h}M\mu_1 - \frac{2e}{h}M\mu_1(1-T) - \frac{2e}{h}M\mu_2 T = \frac{2e}{h}M(\mu_1 - \mu_2)T$$

Total current at lead 2:

$$I_2 = I_2^+ + I_2^- = \frac{2e}{h}M\mu_1 T + \frac{2e}{h}M\mu_2(1-T) - \frac{2e}{h}M\mu_2 = \frac{2e}{h}M(\mu_1 - \mu_2)T$$

Physics of MQT: Not perfect but ballistic conductor

- **Ballistic conductor w/ a single impurity:** size of conductor, $L < L_m$

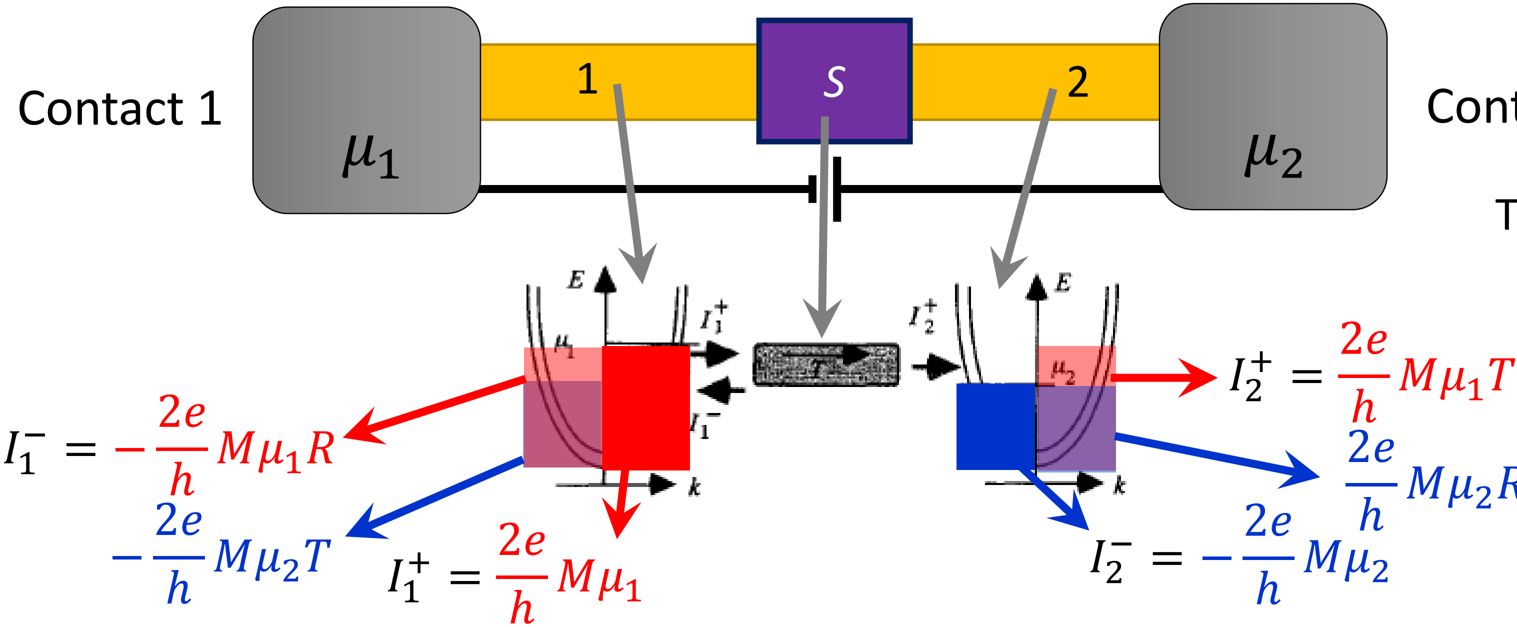

TR symmetry is implied

Total current at lead 1&2:

$$I = I_1 = I_2 = \frac{2e}{h}M(\mu_1 - \mu_2)T = \frac{2e^2}{h}MT\left(\frac{\mu_1 - \mu_2}{e}\right) = \frac{2e^2}{h}MTV$$

$$G = \frac{2e^2}{h}MT$$

Perfect conductor $T = 1$

Physics of MQT: No perfect & diffusive conductor

- **Back to the Ohm's law :** L_m, $L_\varphi << L$, $\lambda_F << W$

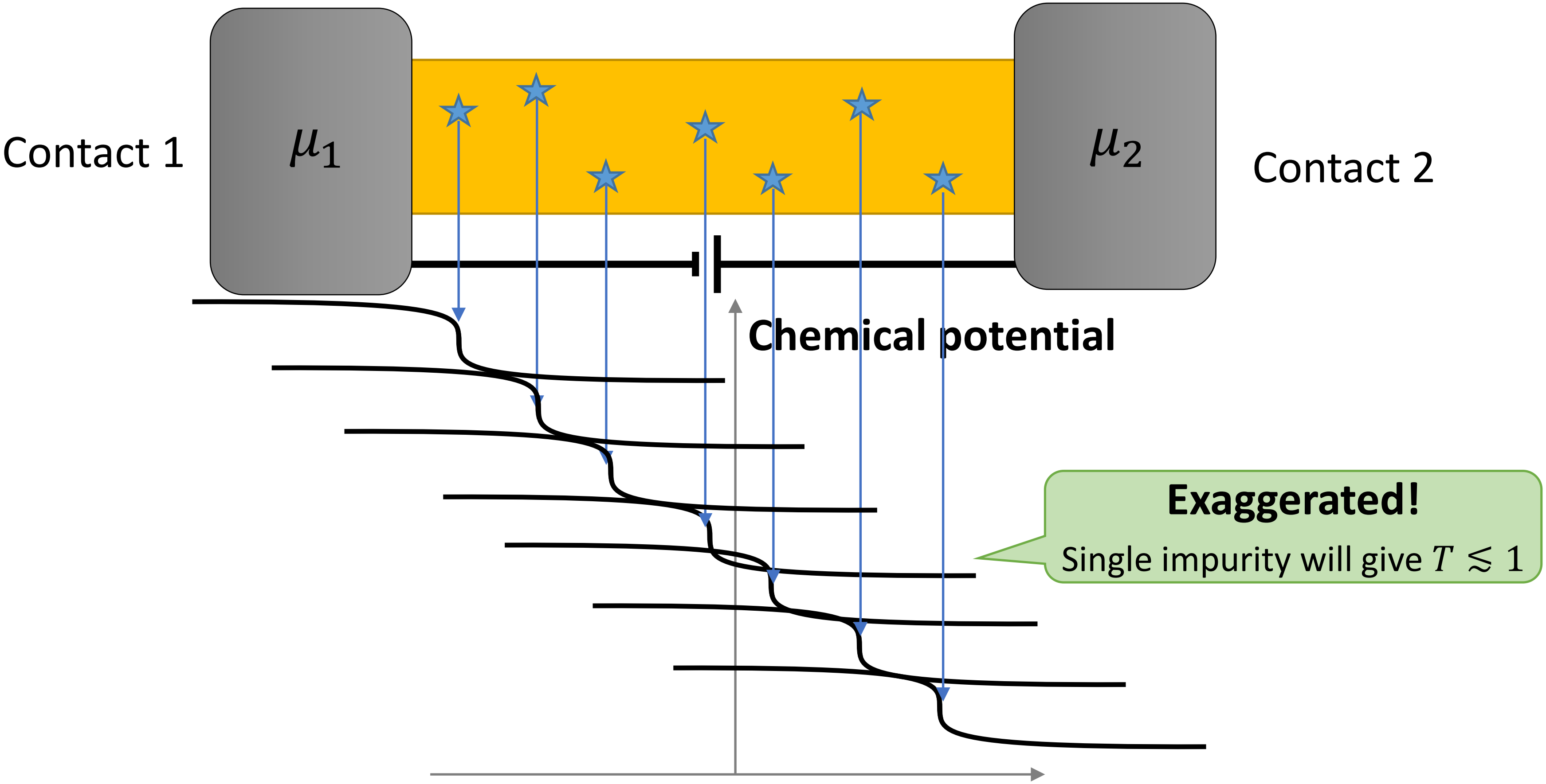

Physics of MQT: No perfect & diffusive conductor

- **Back to the Ohm's law :** L_m, $L_\varphi \ll L$, $\lambda_F \ll W$

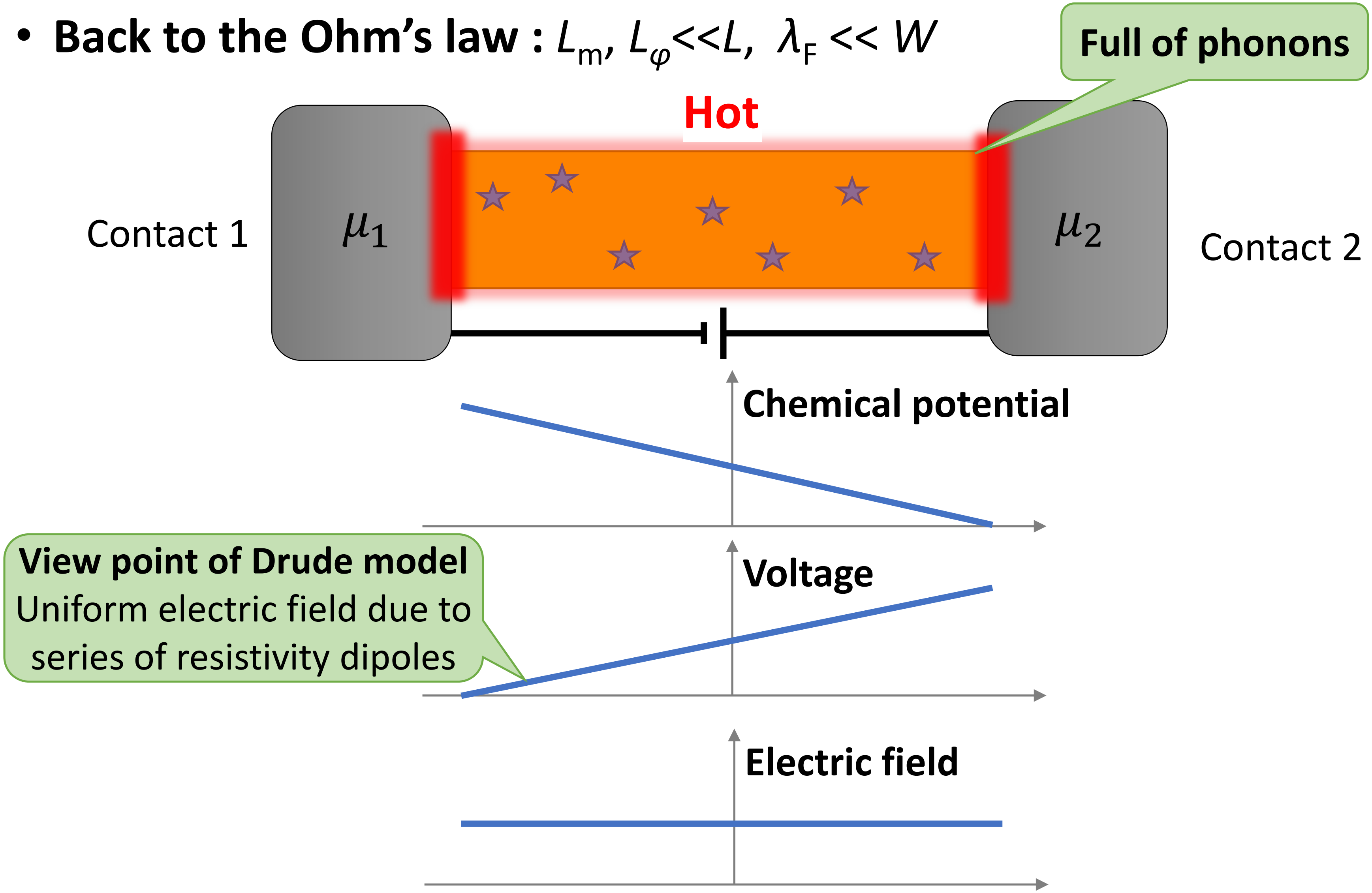

Physics of MQT: Not perfect but ballistic conductor

- **Back to the Ohm's law :** L_m, $L_\varphi << L$, $\lambda_\mathrm{F} << W$

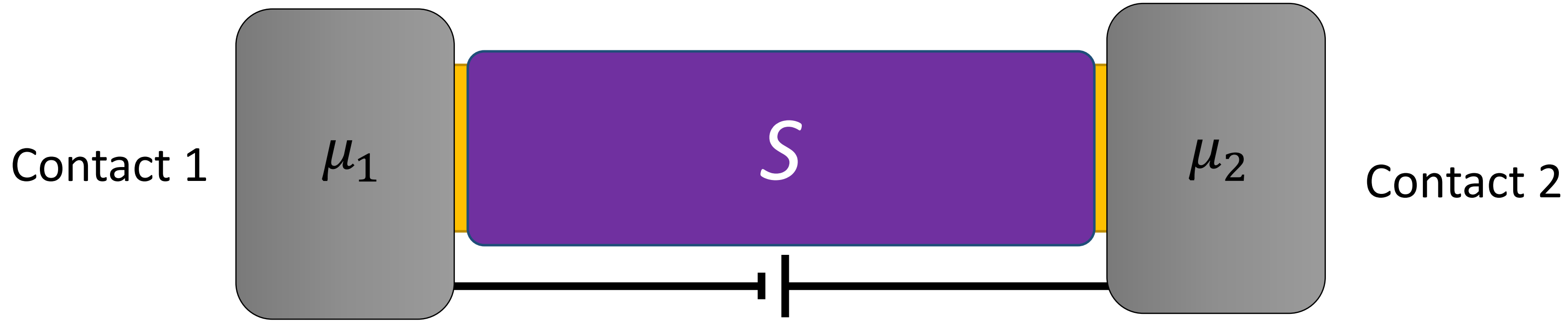

- **Landauer formula for Ohmic regime**

$$\boxed{G = \frac{2e^2}{h} MT}$$

$$M \sim \frac{k_F W}{\pi}$$

$$T(N) \sim \frac{L_\mathrm{m}}{L}$$

$$G = \frac{2e^2}{h}\frac{k_F W}{\pi}\frac{L_\mathrm{m}}{L} = \left(\frac{2e^2 k_F L_\mathrm{m}}{h}\right)\frac{W}{L}$$

$$\sigma = \frac{2e^2 k_F}{h}\frac{h k_F \tau}{2\pi m} = \frac{k_F^2}{\pi}\frac{e^2 \tau}{m} = \frac{ne^2\tau}{m}$$

Ohm's Law & Drude model is derived

(Lesson) Now we know when MQT becomes classical from a microscopic view point & How limited Drude model is.

Landauer formalism gives another lesson:

all you need to know for transport is the S-matrix.

(as long as it is a single particle physics)

Physics of MQT: multi-terminal transport

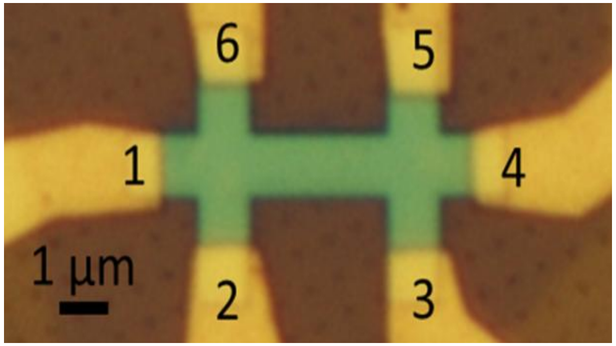

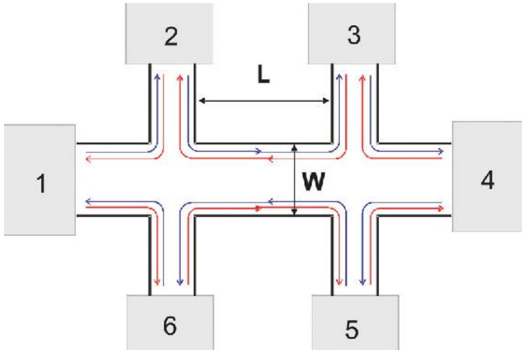

- **Büttiker formula: multi-terminal transport**

$$I_p = \frac{2e}{h}\sum_q\left[T_{q\leftarrow p}\mu_p - T_{p\leftarrow q}\mu_q\right] = \sum_q\left[G_{qp}V_p - G_{pq}V_q\right]$$

c.f. two-terminal case

$T_{21} = T_{12}$ to have $I_1 = 0$ for $\mu_1 - \mu_2$

$G = \dfrac{2e^2}{h}T_{12}$

$$I_1 = \frac{2e}{h}(T_{21}\mu_1 - T_{12}\mu_2) = \frac{2e}{h}T_{12}(\mu_1 - \mu_2) = GV$$

- **Sum rule:** $\sum_q G_{qp} = \sum_q G_{pq}$ to have $I_p = 0$ for $V_p = V_q = V_0$

Physics of MQT: multi-terminal transport

- **Three-terminal case**

$$I_1 = \frac{2e}{h}(T_{21}\mu_1 + T_{31}\mu_1 - T_{12}\mu_2 - T_{13}\mu_3)$$

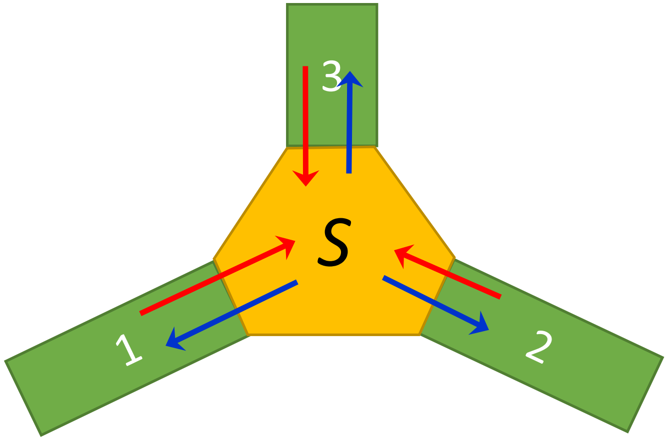

$$S = \begin{pmatrix} s_{11} & s_{12} & s_{13} \\ s_{21} & s_{22} & s_{23} \\ s_{31} & s_{32} & s_{33} \end{pmatrix}$$

$$\begin{pmatrix} B_1 \\ B_2 \\ B_3 \end{pmatrix}_{\mathrm{out}} = \begin{pmatrix} s_{11} & s_{12} & s_{13} \\ s_{21} & s_{22} & s_{23} \\ s_{31} & s_{32} & s_{33} \end{pmatrix} \begin{pmatrix} A_1 \\ A_2 \\ A_3 \end{pmatrix}_{\mathrm{in}}$$

$T_{21} = |s_{ab}|^2$, a & b = ?

Physics of MQT: multi-terminal transport

- **Three-terminal case**

$$I_1 = \frac{2e}{h}(T_{21}\mu_1 + T_{31}\mu_1 - T_{12}\mu_2 - T_{13}\mu_3)$$

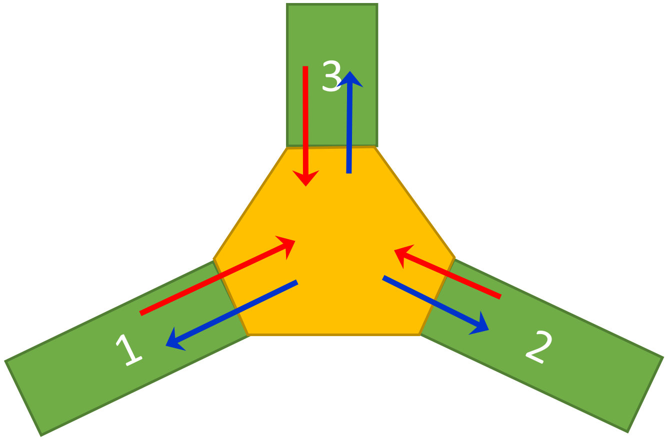

$$S = \begin{pmatrix} s_{11} & s_{12} & s_{13} \\ s_{21} & s_{22} & s_{23} \\ s_{31} & s_{32} & s_{33} \end{pmatrix}$$

$$\begin{pmatrix} B_1 \\ B_2 \\ B_3 \end{pmatrix}_{\text{out}} = \begin{pmatrix} s_{11} & s_{12} & s_{13} \\ s_{21} & s_{22} & s_{23} \\ s_{31} & s_{32} & s_{33} \end{pmatrix} \begin{pmatrix} A_1 \\ A_2 \\ A_3 \end{pmatrix}_{\text{in}}$$

$$T_{21} = |s_{21}|^2$$

$$\begin{aligned} I_1 &= \frac{2e}{h}(T_{21}\mu_1 + T_{31}\mu_1 - T_{12}\mu_2 - T_{13}\mu_3) \\ &= G_{21}\mu_1 + G_{31}\mu_1 - G_{12}\mu_2 - G_{13}\mu_3 \\ &= G_{21}(V_1 - V_2) + G_{31}(V_1 - V_3) \end{aligned}$$

$I_1 = -I_3 - I_2$ (Kirchhoff's Law)

Try!

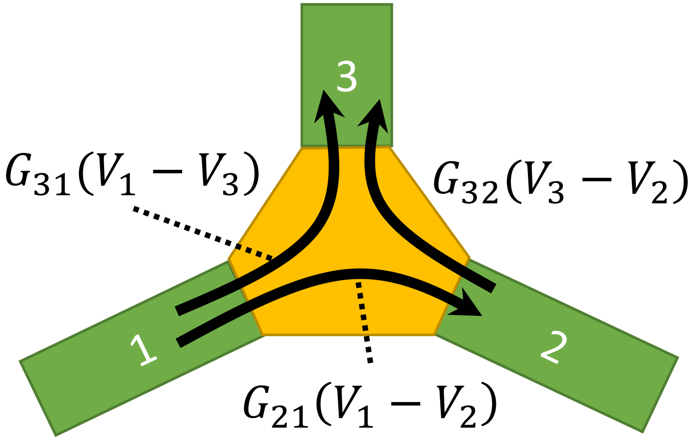

Physics of MQT: finite voltage bias and temperature

- **Beyond the linear response regime: Kubo's formula is not enough**

  → *S*-matrix, energy-dependent

  → Non-zero temperature

$$I = \frac{2e}{h} MT(\mu_1 - \mu_2) = \frac{2e}{h} MT \int [f_1(E) - f_2(E)] dE$$

$$\mapsto \frac{2e}{h} \sum_n \int T_n(E)[f_1(E) - f_2(E)] dE$$

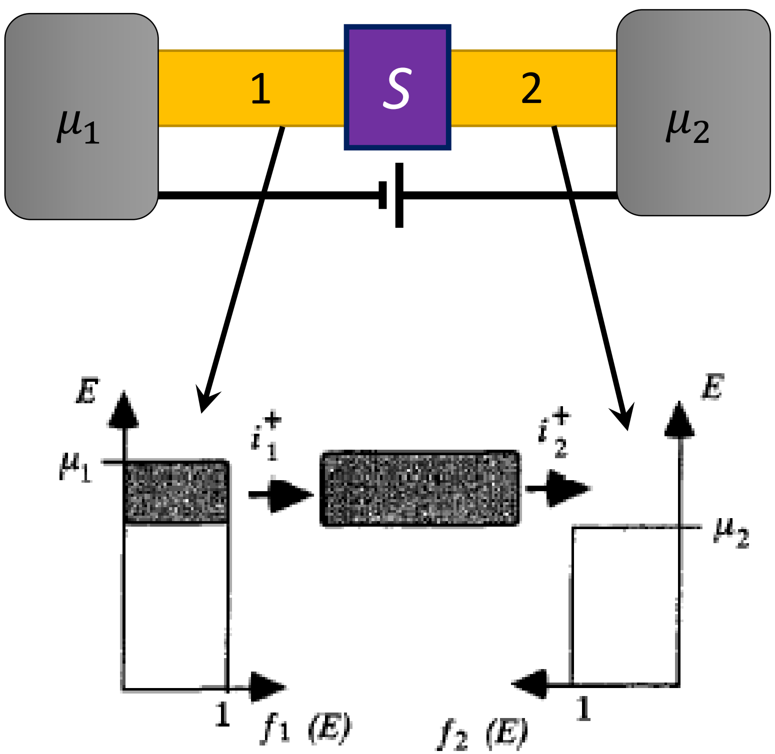

Thermoelectric transport
can be dealt

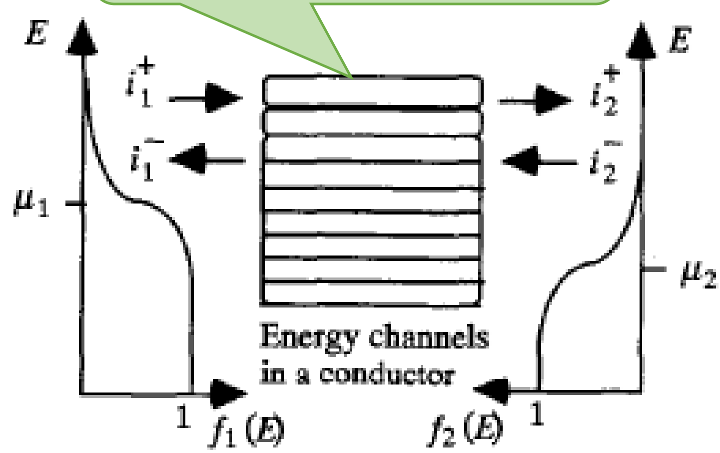

Application of Landauer-Büttiker formalism

- **Usages of Landauer-Büttiker formalism in research (analytical)**

  → **Universal physics**: precise S-matrix may not be required much

  → **Symmetry**: S-matrix can be known solely from symmetry

Resonant tunneling in MQT is universal in that particular shapes $V(x)$ or materials do not matter

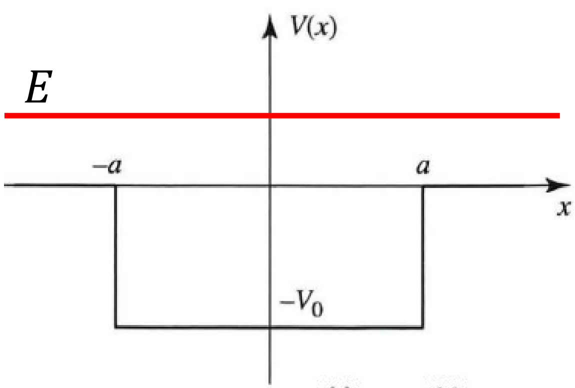

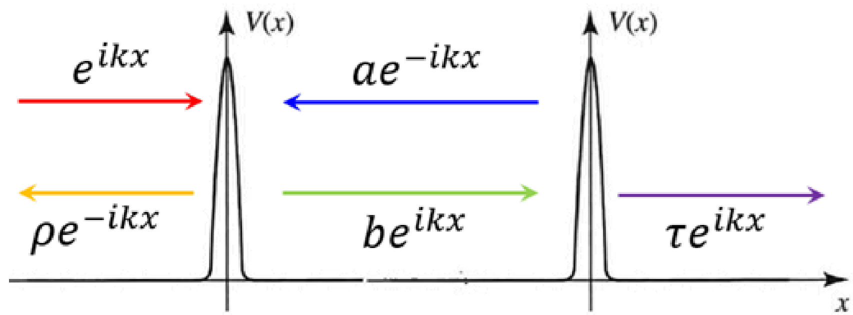

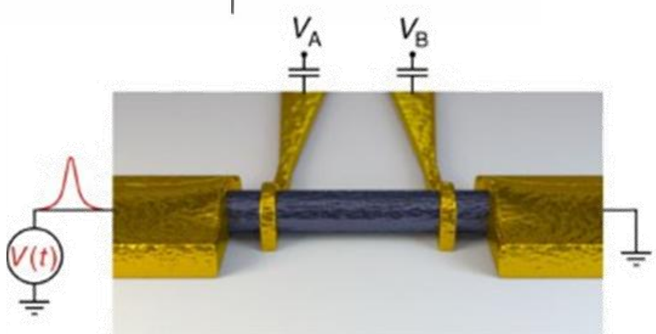

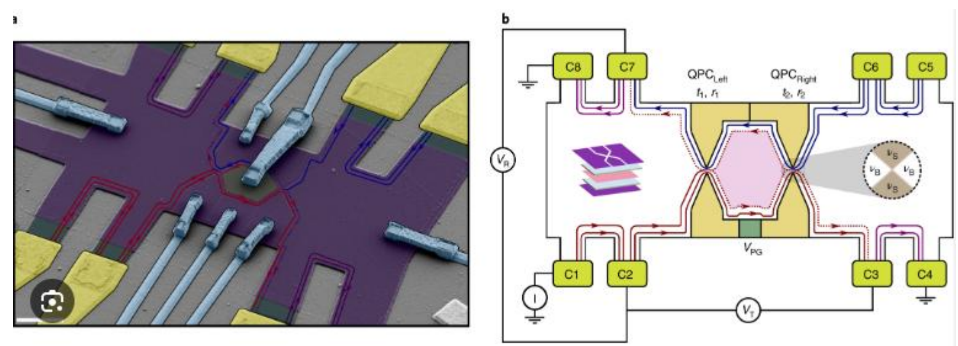

Beyond coherent & metallic conductions

- **More about Landauer-Büttiker formalism**

  → MQT is quantal: DC current = $\langle \hat{I} \rangle$, i.e., long-time average of current

  → Current shot noise is also available [M. Büttiker, *PRB* **46**, 12485 (1992)]

  → Periodically driven quantum pumps can be dealt [M. Büttiker, (1990)]

- **Beyond Landauer-Büttiker formalism: other methods for MQT**

Formalisms	Advantages	Disadvantages
Landauer-Büttiker	Intuitive & quick calculations. Finite voltage bias & temperature	Cannot deal with many-body physics
Kubo's linear response theory	Relatively easy & quick, while allowing many-body physics	Only allows physics around equilibrium states
Master equation	Allowing many-body physics & Nonequilibrium bias & finite temp.	Particularly useful at tunneling regime
Keldysh formalism	All the above	Not so easy for everyone

Overview

- **Recap. of the last lecture: Mesoscopic Quantum Transport (MQT)**

  → It has been exactly 1 year!

- **MQT and low-energy theory w/ mesoscopic interactions**

  → Low-energy effective theory by $\vec{k} \cdot \vec{p}$-method

- **$\vec{k} \cdot \vec{p}$-method & Mesoscopic Interactions in action**

  → Spin-orbit, electric & magnetic field, superconducting order

- **MQT in action**

  → $\frac{dI}{dV}$ of topological systems calculating S-matrix

- **What left beyond today's lecture**

Mesoscopic Quantum Transport in 2 hours!

- **MQT in condensed matter systems under interactions**?

→ Landauer-Büttiker formalism: S-matrix is the central quantity!

$$I = \frac{2e}{h}\sum\nolimits_n \int T(E)[f_1(E) - f_2(E)]dE$$

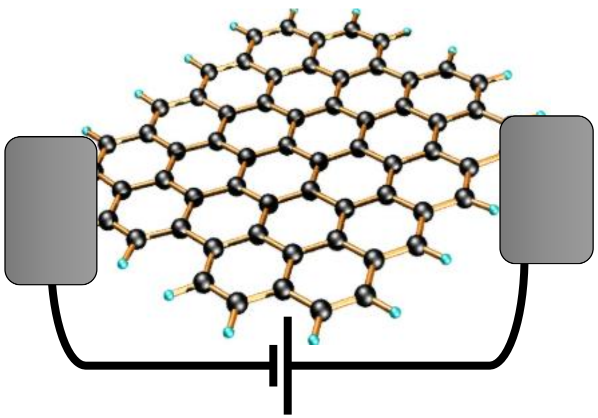

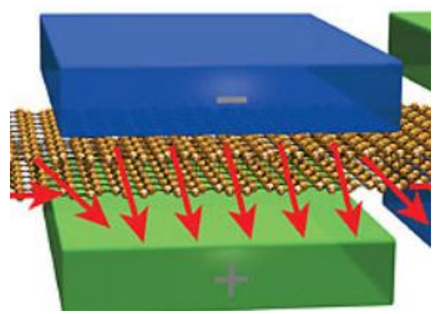

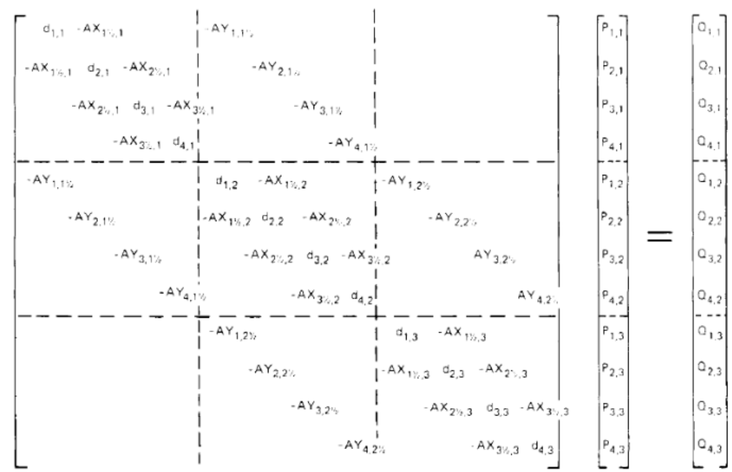

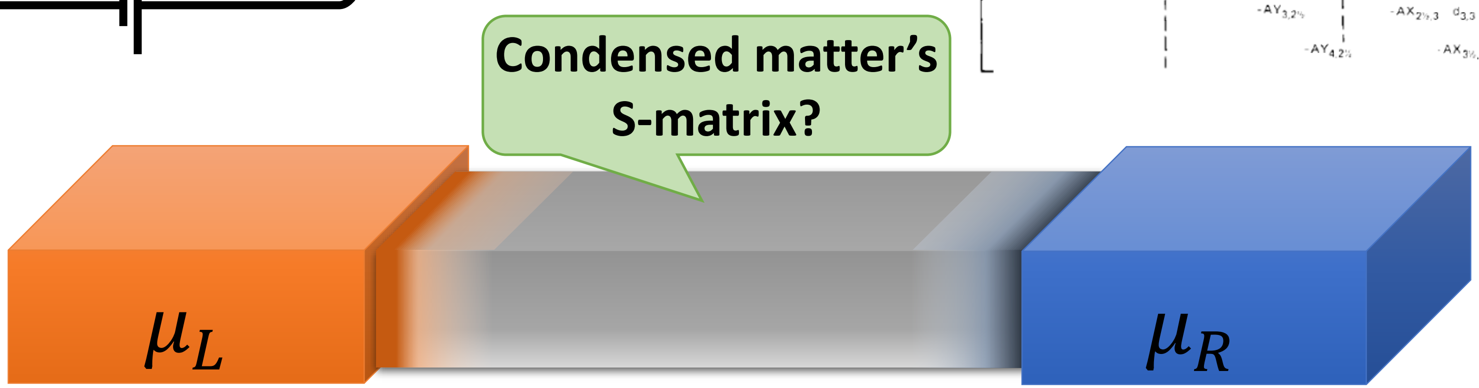

MQT: scales matter always

- **MQT in condensed matter systems under interactions**?

→ Current at (nearly) zero temp.

$$I = I(V) = \frac{2e}{h}\int_{\mu_R}^{\mu_L} T(E)dE$$

S-matrix only around particular energies

→ Differential conductance at (nearly) zero temp.

$$\frac{dI}{dV} = \frac{I(V+dV)-I(V)}{dV} = \frac{2e^2}{h}T(\mu_L)$$

Yields selected quantum propagations

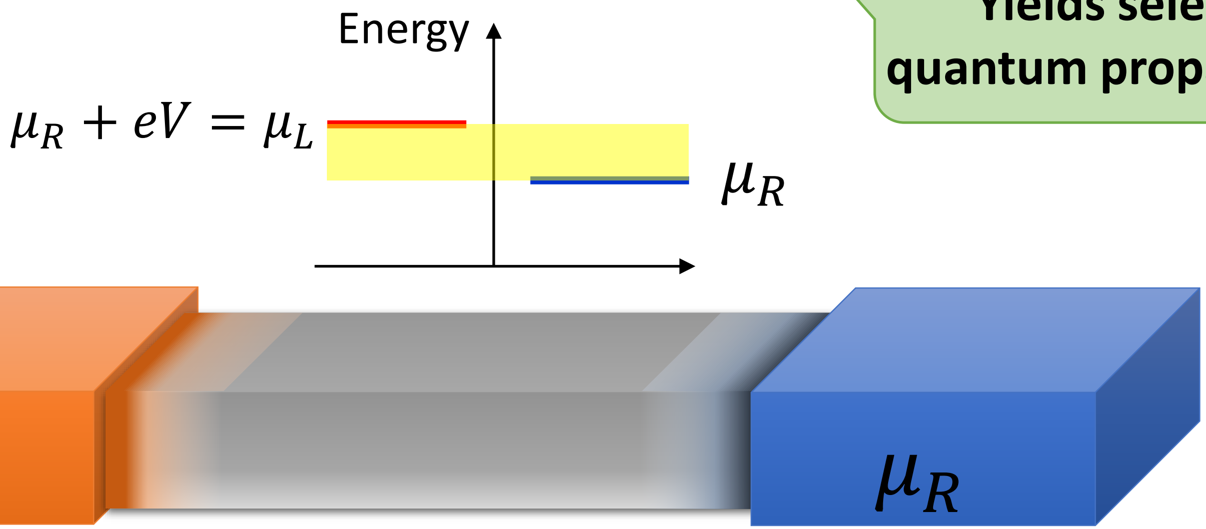

MQT and low-energy theory w/ mesoscopic interactions

- **Low-energy effective Hamiltonian**

  → In the case of graphene

a

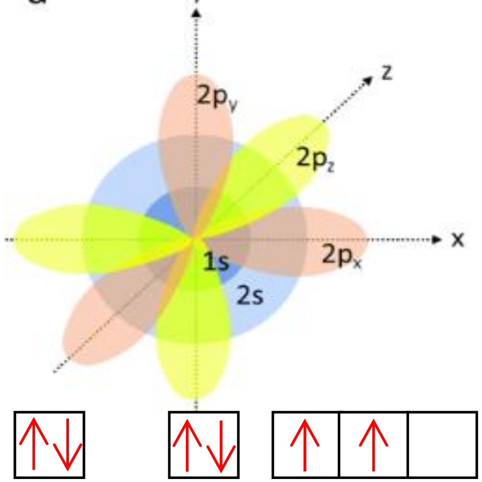

n=1	n=2	n=2
l=0	l=0	l=1
1s	2s	$2p_{x,y,z}$

<Top view>

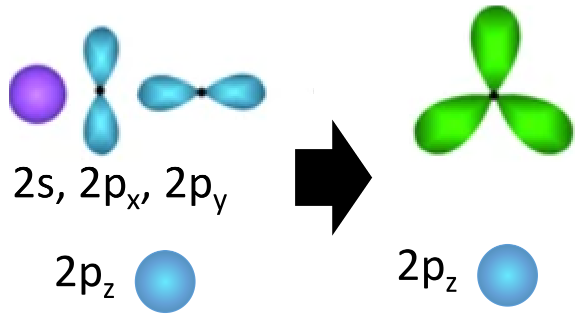

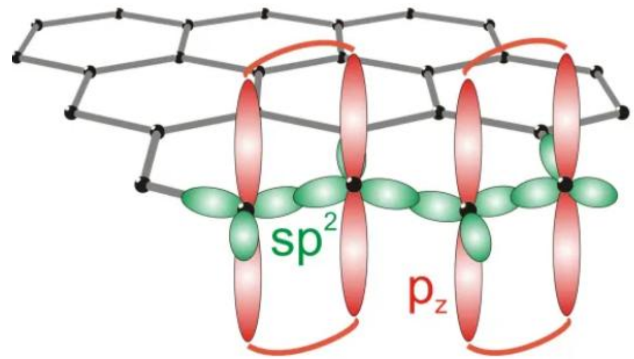

n=2

n=1

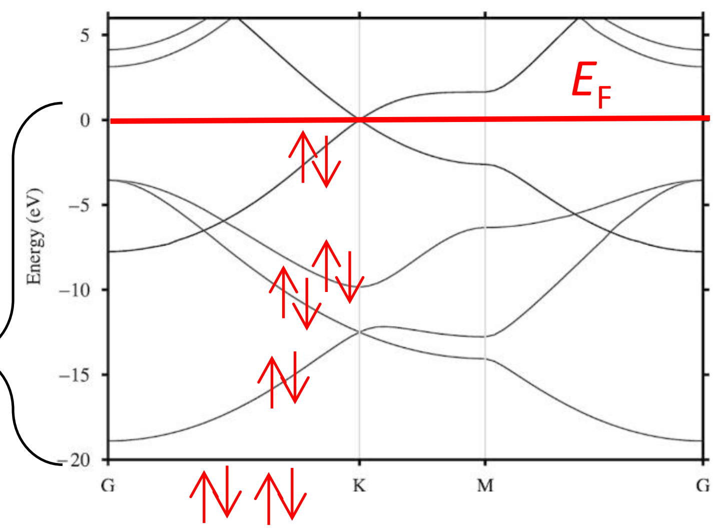

12 electrons in unit cell

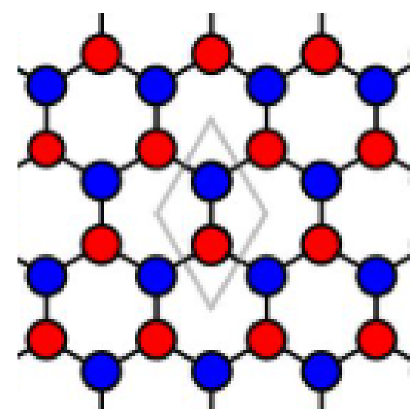

MQT and low-energy theory w/ mesoscopic interactions

- **Low-energy effective Hamiltonian**

  → In the case of graphene

Conduction occurs around this energy

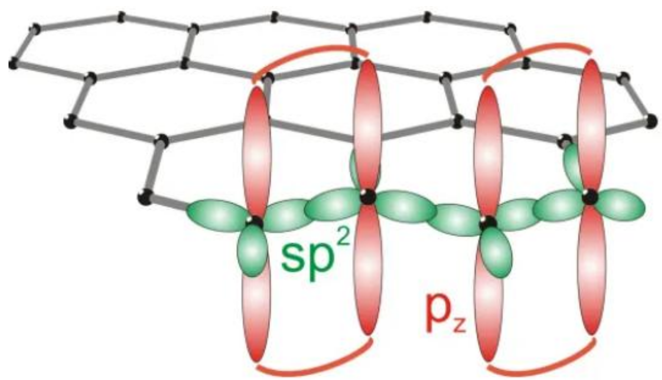

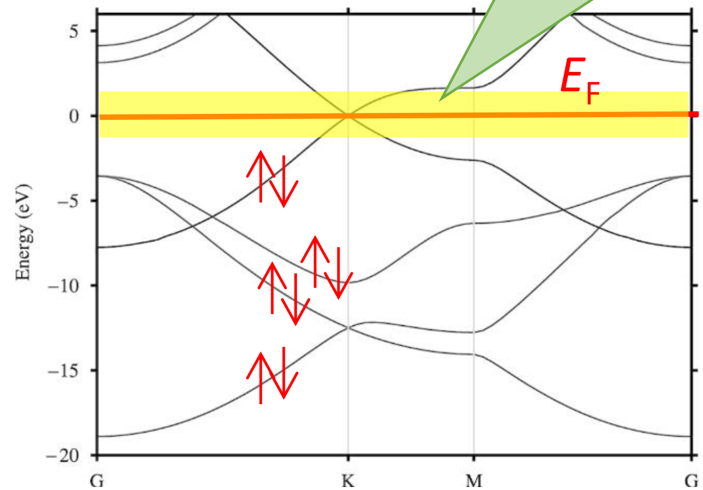

Around E_F

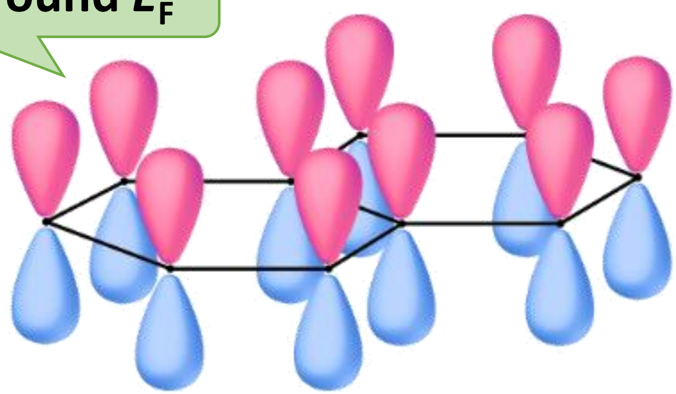

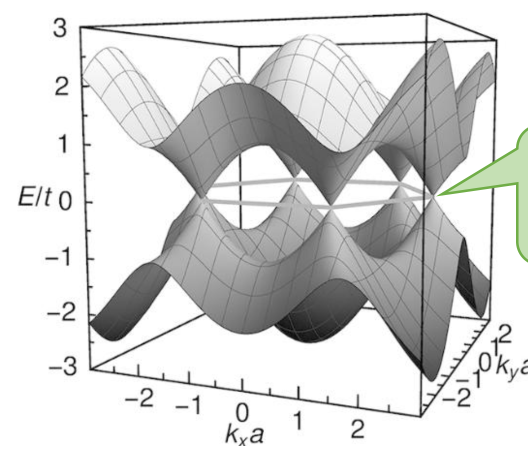

2D Dirac Fermions

MQT and low-energy theory w/ mesoscopic interactions

- **Low-energy effective Hamiltonian**

  → In the case of graphene

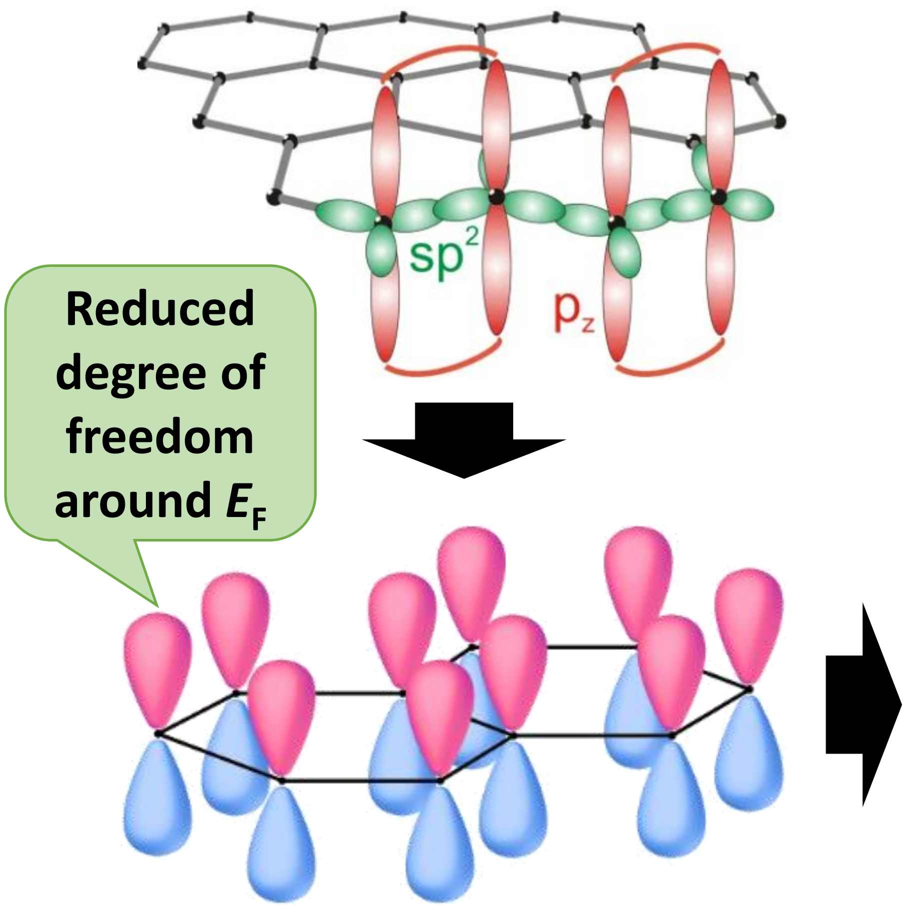

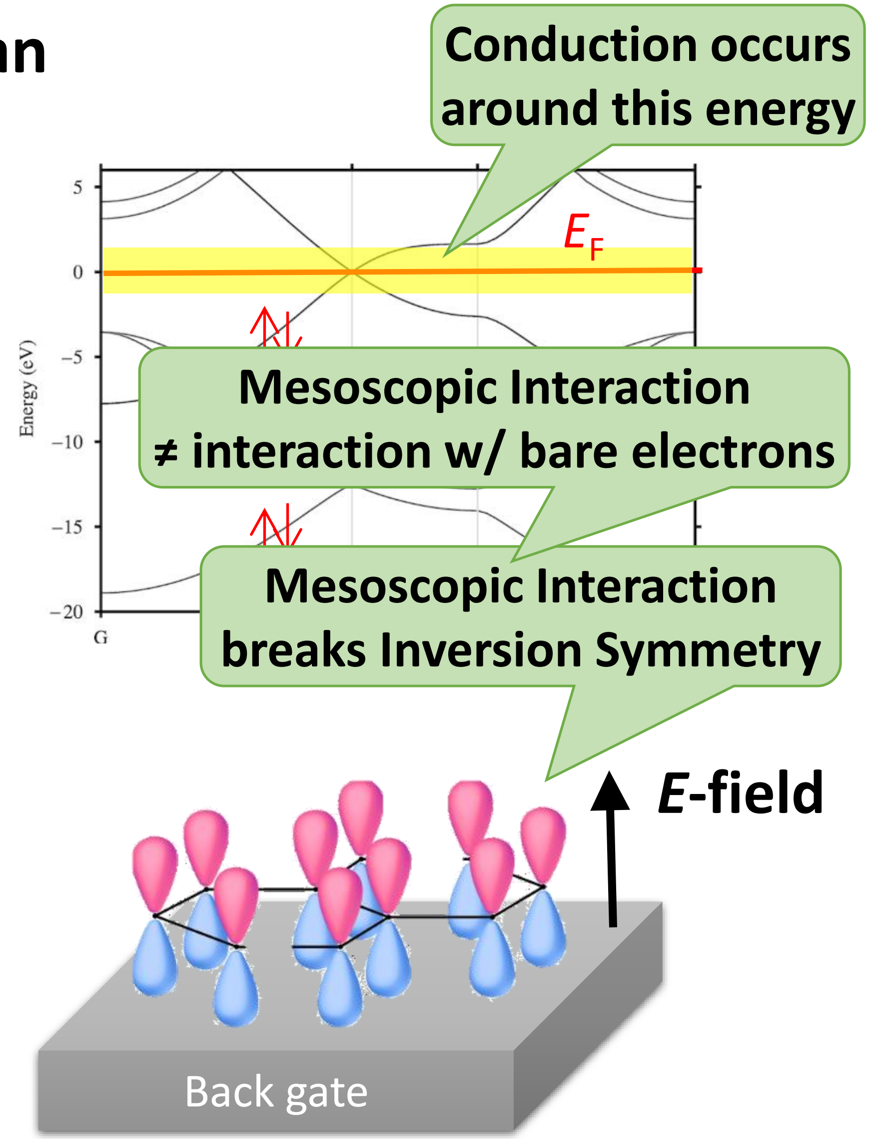

- **Low-energy effective Hamiltonian**

  → In the case of WSe_2, 2D Transition Metal Dichalcogenides (TMD)

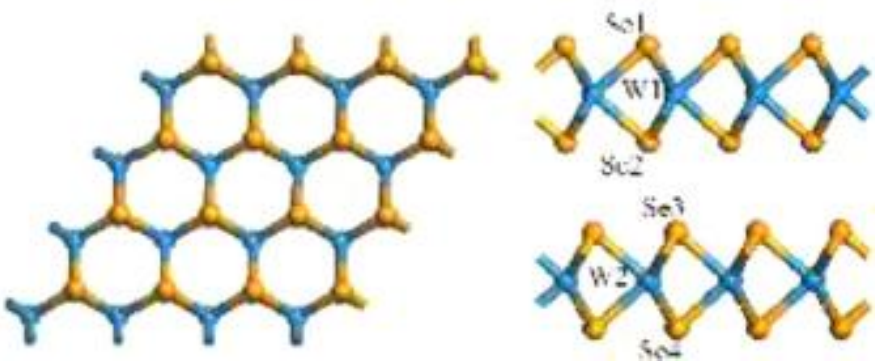

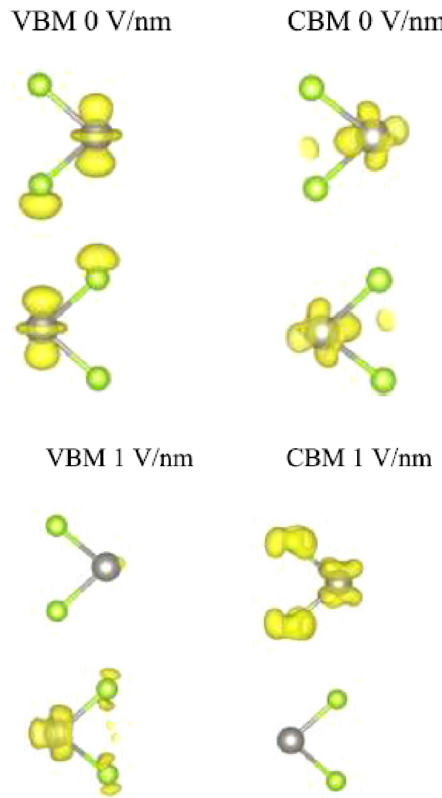

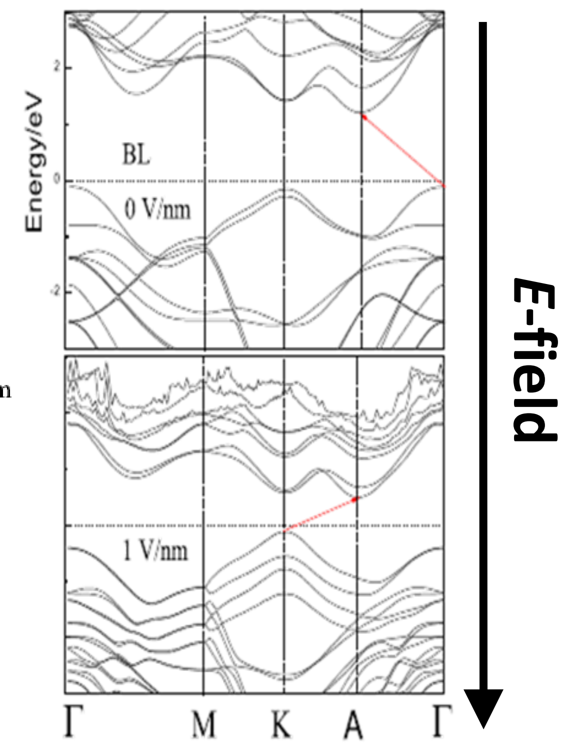

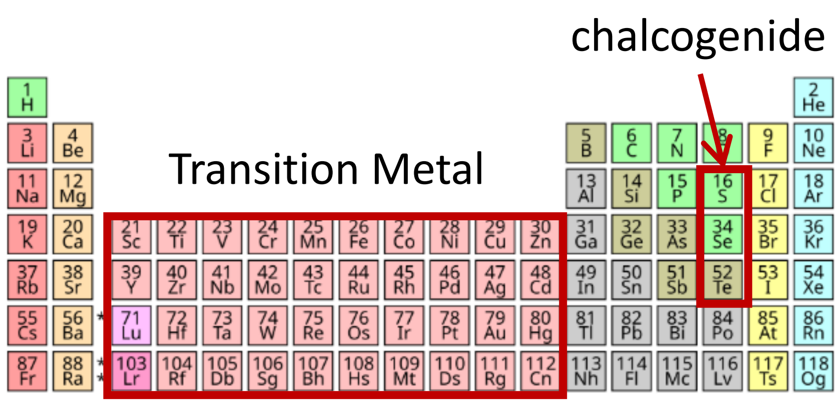

JOURNAL OF APPLIED PHYSICS **117**, 084310 (2015)

$\vec{k} \cdot \vec{p}$-method in action: formalism

- **Low-energy effective Hamiltonian:** $\vec{k} \cdot \vec{p}$-method

  → How does a system looks around a particular momentum

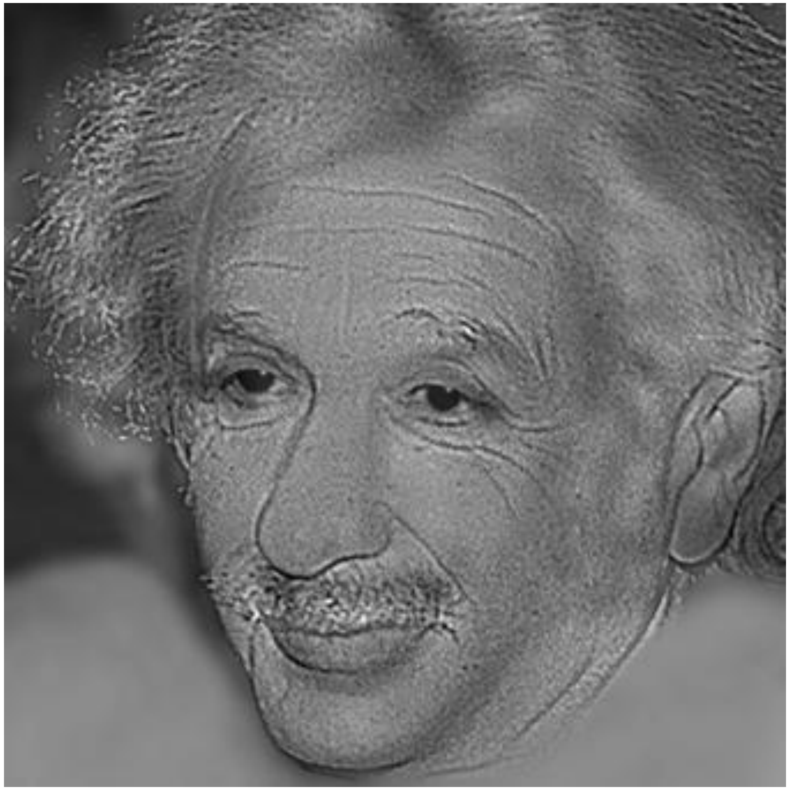

Around large *k* this looks →

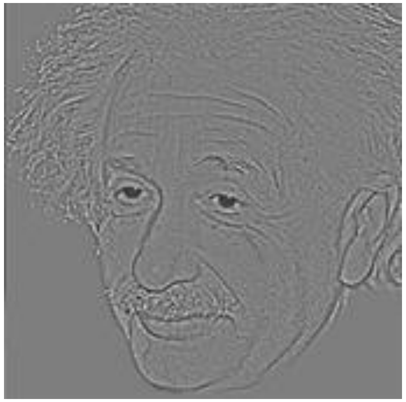

Around small *k* this looks →

$\vec{k} \cdot \vec{p}$-method in action: formalism

- **Low-energy effective Hamiltonian:** $\vec{k} \cdot \vec{p}$-method

  → How does a system looks around a particular momentum $\vec{k}$

  → There will be eigenstates $\left|n\vec{k}\right\rangle$ of the full Hamiltonian $\widehat{H}$

$$\widehat{H}\left(\vec{k}\right)\left|n\vec{k}\right\rangle = E_n\left(\vec{k}\right)\left|n\vec{k}\right\rangle$$

  → Select subspace of the full Hilbert space with *n*'s such that

  $E_n\left(\vec{k}\right)$ is around Fermi energy. Let's say those are *n*=1,2

  → Matrix representation of the low-energy Hamiltonian around E_F

$$\widehat{H}_{\text{eff}}(\vec{p}) = \begin{pmatrix} \left\langle 1\vec{k}\middle|\widehat{H}(\vec{k}+\vec{p})\middle|1\vec{k}\right\rangle & \left\langle 1\vec{k}\middle|\widehat{H}(\vec{k}+\vec{p})\middle|2\vec{k}\right\rangle \\ \left\langle 2\vec{k}\middle|\widehat{H}(\vec{k}+\vec{p})\middle|1\vec{k}\right\rangle & \left\langle 2\vec{k}\middle|\widehat{H}(\vec{k}+\vec{p})\middle|2\vec{k}\right\rangle \end{pmatrix}$$

You can choose n's as many as you want

$\vec{k} \cdot \vec{p}$-method in action: formalism

- **Low-energy effective Hamiltonian:** $\vec{k} \cdot \vec{p}$-method

$$\hat{H}_{\text{eff}}(\vec{p}) = \begin{pmatrix} \langle 1\vec{k}|\hat{H}(\vec{k}+\vec{p})|1\vec{k}\rangle & \langle 1\vec{k}|\hat{H}(\vec{k}+\vec{p})|2\vec{k}\rangle \\ \langle 2\vec{k}|\hat{H}(\vec{k}+\vec{p})|1\vec{k}\rangle & \langle 2\vec{k}|\hat{H}(\vec{k}+\vec{p})|2\vec{k}\rangle \end{pmatrix}$$

- **Philosophy behind** $\vec{k} \cdot \vec{p}$-method

→ Put $\vec{p} = 0$

$$\hat{H}_{\text{eff}}(0) = \begin{pmatrix} \langle 1\vec{k}|\hat{H}(\vec{k})|1\vec{k}\rangle & \langle 1\vec{k}|\hat{H}(\vec{k})|2\vec{k}\rangle \\ \langle 2\vec{k}|\hat{H}(\vec{k})|1\vec{k}\rangle & \langle 2\vec{k}|\hat{H}(\vec{k})|2\vec{k}\rangle \end{pmatrix} = \begin{pmatrix} E_{1\vec{k}} & 0 \\ 0 & E_{2\vec{k}} \end{pmatrix}$$

Exact

→ If $\vec{p}$ is small,

$$|n, \vec{k}+\vec{p}\rangle \approx |n, \vec{k}\rangle$$

1st order Perturbation
(2nd order is often used)

→ Accordingly,

$$\hat{H}_{\text{eff}}(\vec{p}) = \begin{pmatrix} \langle 1\vec{k}|\hat{H}(\vec{k}+\vec{p})|1\vec{k}\rangle & \langle 1\vec{k}|\hat{H}(\vec{k}+\vec{p})|2\vec{k}\rangle \\ \langle 2\vec{k}|\hat{H}(\vec{k}+\vec{p})|1\vec{k}\rangle & \langle 2\vec{k}|\hat{H}(\vec{k}+\vec{p})|2\vec{k}\rangle \end{pmatrix}$$

$\vec{k} \cdot \vec{p}$-method in action: Low-energy effective *H*

- **2D Transition Metal Dichalcogenides**

  → PRL **108**, 196802 (2012)

Coupled Spin and Valley Physics in Monolayers of MoS2 and Other Group-VI Dichalcogenides

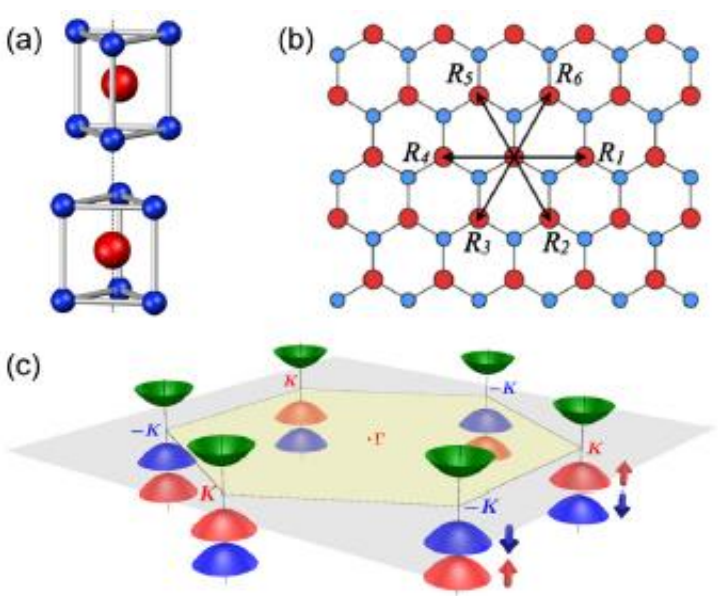

FIG. 1 (color online). (a) The unit cell of bulk $2H$-MoS_2, which has the inversion center located in the middle plane. It contains two unit cells of MoS_2 monolayers, which lacks an inversion center. (b) Top view of the MoS_2 monolayer. $\boldsymbol{R}_i$ are the vectors connecting nearest Mo atoms. (c) Schematic drawing of the band structure at the band edges located at the K points.

shown in Fig. 1(c). The group of the wave vector at the band edges (K) is C_{3h} and the symmetry adapted basis functions are

$$|\phi_c\rangle = |d_{z^2}\rangle, \qquad |\phi_v^\tau\rangle = \frac{1}{\sqrt{2}}(|d_{x^2-y^2}\rangle + i\tau|d_{xy}\rangle), \quad (1)$$

$\tau = 1(-1)$ for *K(K')*-valley

To first order in k, the C_{3h} symmetry dictates that the two-band $k \cdot p$ Hamiltonian has the form

$$\hat{H}_0 = at(\tau \boxed{k_x}\hat{\sigma}_x + \boxed{k_y}\hat{\sigma}_y) + \frac{\Delta}{2}\hat{\sigma}_z, \quad (2)$$

state splits. Approximating the SOC by the intra-atomic contribution $\boldsymbol{L} \cdot \boldsymbol{S}$, we find the total Hamiltonian given by

$$\hat{H} = at(\tau k_x\hat{\sigma}_x + k_y\hat{\sigma}_y) + \frac{\Delta}{2}\hat{\sigma}_z \boxed{- \lambda\tau\frac{\hat{\sigma}_z - 1}{2}\hat{s}_z}, \quad (3)$$

Mesoscopic interaction

where 2λ is the spin splitting at the valence band top caused by the SOC and $\hat{s}_z$ is the Pauli matrix for spin.

$\vec{k} \cdot \vec{p}$-method in action: Low-energy effective *H*

- **2D Transition Metal Dichalcogenides**

  → PRL **108**, 196802 (2012)

Coupled Spin and Valley Physics in Monolayers of MoS2 and Other Group-VI Dichalcogenides

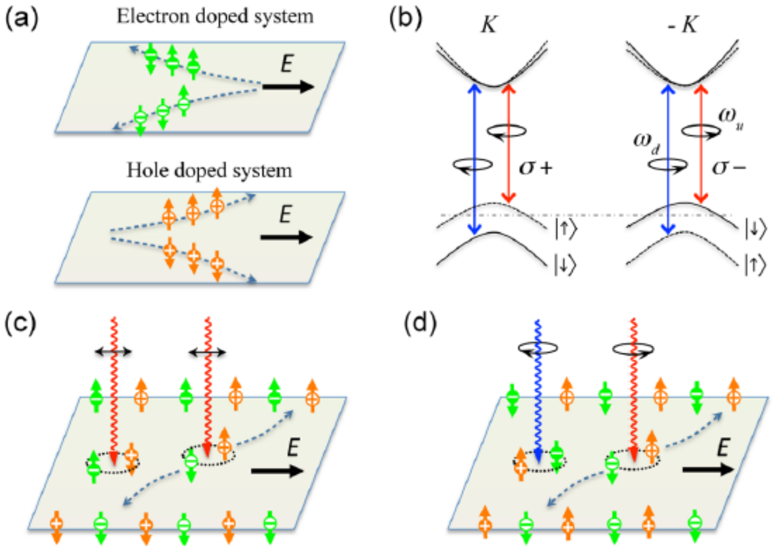

$$\Omega_c(\boldsymbol{k}) = -\tau \frac{2a^2t^2\Delta'}{[\Delta'^2 + 4a^2t^2k^2]^{3/2}}.$$

shown in Fig. 1(c). The group of the wave vector at the band edges (K) is C_{3h} and the symmetry adapted basis functions are

$$|\phi_c\rangle = |d_{z^2}\rangle, \qquad |\phi_v^\tau\rangle = \frac{1}{\sqrt{2}}(|d_{x^2-y^2}\rangle + i\tau|d_{xy}\rangle), \quad (1)$$

$\tau = 1(-1)$ for *K(K')*-valley

To first order in k, the C_{3h} symmetry dictates that the two-band $k \cdot p$ Hamiltonian has the form

$$\hat{H}_0 = at(\tau \boxed{k_x} \hat{\sigma}_x + \boxed{k_y} \hat{\sigma}_y) + \frac{\Delta}{2}\hat{\sigma}_z, \qquad (2)$$

state splits. Approximating the SOC by the intra-atomic contribution $\boldsymbol{L} \cdot \boldsymbol{S}$, we find the total Hamiltonian given by

$$\hat{H} = at(\tau k_x \hat{\sigma}_x + k_y \hat{\sigma}_y) + \frac{\Delta}{2}\hat{\sigma}_z \boxed{- \lambda\tau \frac{\hat{\sigma}_z - 1}{2}\hat{s}_z}, \qquad (3)$$

Mesoscopic interaction

where 2λ is the spin splitting at the valence band top caused by the SOC and $\hat{s}_z$ is the Pauli matrix for spin.

$\vec{k} \cdot \vec{p}$-method in action: Low-energy effective H

- **2D Transition Metal Dichalcogenides**

  → PRL **108**, 196802 (2012)

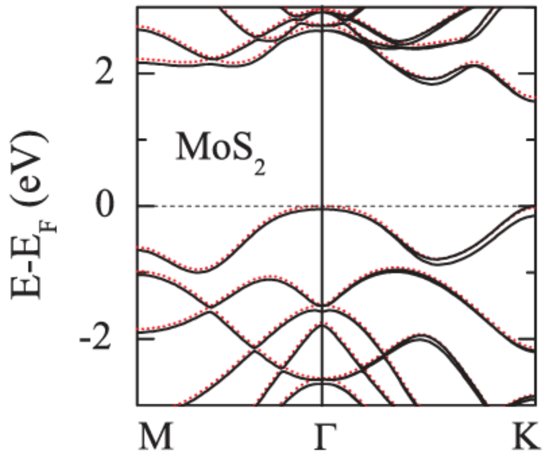

TABLE I. Fitting result from first-principles band structure calculations. The monolayer is relaxed. The sizes of spin splitting 2λ at valence-band edge were previously reported in the first principle studies [12]. The unit is Å for a, and eV for t, Δ, and λ. Ω_1 (Ω_2) is the Berry curvature in unit of Å^2, evaluated at $-K$ point for the spin-up (-down) conduction band.

	a	Δ	t	2λ	Ω_1	Ω_2
MoS_2	3.193	1.66	1.10	0.15	9.88	8.26
WS_2	3.197	1.79	1.37	0.43	15.51	9.57
$MoSe_2$	3.313	1.47	0.94	0.18	10.23	7.96
WSe_2	3.310	1.60	1.19	0.46	16.81	9.39

shown in Fig. 1(c). The group of the wave vector at the band edges (K) is C_{3h} and the symmetry adapted basis functions are

$$|\phi_c\rangle = |d_{z^2}\rangle, \qquad |\phi_v^\tau\rangle = \frac{1}{\sqrt{2}}(|d_{x^2-y^2}\rangle + i\tau|d_{xy}\rangle), \quad (1)$$

$\tau = 1(-1)$ for *K(K')*-valley To first order in k, the C_{3h} symmetry dictates that the two-band $k \cdot p$ Hamiltonian has the form

$$\hat{H}_0 = at(\tau k_x \hat{\sigma}_x + k_y \hat{\sigma}_y) + \frac{\Delta}{2}\hat{\sigma}_z, \quad (2)$$

state splits. Approximating the SOC by the intra-atomic contribution $\boldsymbol{L} \cdot \boldsymbol{S}$, we find the total Hamiltonian given by

$$\hat{H} = at(\tau k_x \hat{\sigma}_x + k_y \hat{\sigma}_y) + \frac{\Delta}{2}\hat{\sigma}_z - \lambda\tau\frac{\hat{\sigma}_z - 1}{2}\hat{s}_z, \quad (3)$$

where 2λ is the spin splitting at the valence band top caused by the SOC and $\hat{s}_z$ is the Pauli matrix for spin.

$\vec{k} \cdot \vec{p}$-method in action: Low-energy effective H

- **2D Transition Metal Dichalcogenides**

  → PRL **108**, 196802 (2012)

Counting Symmetry

e.g., Time-reversal symmetry

$$\hat{\Theta} = i\hat{\sigma}_y K? \; \left[\hat{H}_0, \hat{\Theta}\right] = 0?$$

$$\hat{\Theta}^{-1}\hat{H}_0^{\tau}\hat{\Theta} = \hat{\sigma}_y\left(\hat{H}_0^{\tau}\right)^*\hat{\sigma}_y = \hat{H}_0^{-\tau}?$$

where $\hat{\Theta}^{-1} = -i\hat{\sigma}_y K$.

$$\hat{\sigma}_y\left(\hat{H}_0^{\tau}\right)^*\hat{\sigma}_y =$$

$$\hat{\sigma}_y\left[at\left(-i\tau\partial_x\hat{\sigma}_x - i\partial_y\hat{\sigma}_y\right) + \frac{\Delta}{2}\hat{\sigma}_z\right]^*\hat{\sigma}_y$$

$$= \hat{\sigma}_y\left[at\left(i\tau\partial_x\hat{\sigma}_x - i\partial_y\hat{\sigma}_y\right) + \frac{\Delta}{2}\hat{\sigma}_z\right]\hat{\sigma}_y$$

$$= at\left(-i\tau\partial_x\hat{\sigma}_x - i\partial_y\hat{\sigma}_y\right) - \frac{\Delta}{2}\hat{\sigma}_z \neq \hat{H}_0^{-\tau}$$

shown in Fig. 1(c). The group of the wave vector at the band edges (K) is C_{3h} and the symmetry adapted basis functions are

$$|\phi_c\rangle = |d_{z^2}\rangle, \qquad |\phi_v^{\tau}\rangle = \frac{1}{\sqrt{2}}(|d_{x^2-y^2}\rangle + i\tau|d_{xy}\rangle), \qquad (1)$$

$\tau = 1(-1)$ for $K(K')$-valley

To first order in k, the C_{3h} symmetry dictates that the two-band $k \cdot p$ Hamiltonian has the form

$$\hat{H}_0 = at(\tau k_x\hat{\sigma}_x + k_y\hat{\sigma}_y) + \frac{\Delta}{2}\hat{\sigma}_z, \qquad (2)$$

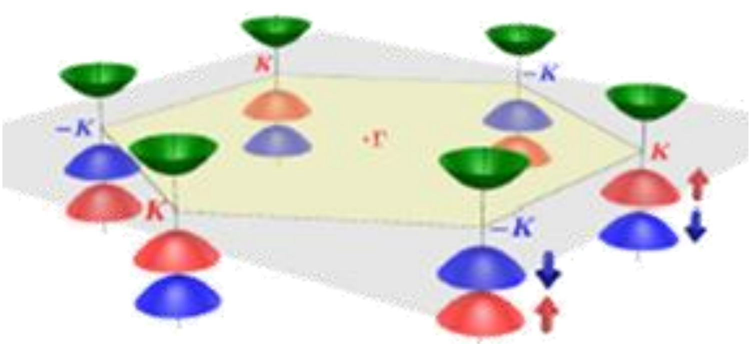

$\vec{k} \cdot \vec{p}$-method in action: Low-energy effective *H*

- **2D Transition Metal Dichalcogenides**

  → PRL **108**, 196802 (2012)

Counting Symmetry

e.g., Time-reversal symmetry $\hat{\Theta} = i\hat{\sigma}_y K$ is not so correct, $\hat{\sigma}$'s are about orbitals. Hence, $\hat{\Theta} \mapsto K$ with $\hat{\Theta}^2 = 1$. See

$$\hat{\Theta}|\phi_v^{\tau}\rangle = |\phi_v^{-\tau}\rangle.$$

Now,

$$\hat{\Theta}^{-1}\hat{H}_0^{\tau}\hat{\Theta} = \left[at\left(-i\tau\partial_x\hat{\sigma}_x - i\partial_y\hat{\sigma}_y\right) + \frac{\Delta}{2}\hat{\sigma}_z\right]^*$$

$$= at\left(-i(-\tau)\partial_x\hat{\sigma}_x - i\partial_y\hat{\sigma}_y\right) + \frac{\Delta}{2}\hat{\sigma}_z$$

$$= \hat{H}_0^{-\tau}$$

Time-reversal of low-energy H of *K*-valley is that of *K'*-valley

shown in Fig. 1(c). The group of the wave vector at the band edges (K) is C_{3h} and the symmetry adapted basis functions are

$$|\phi_c\rangle = |d_{z^2}\rangle, \qquad |\phi_v^{\tau}\rangle = \frac{1}{\sqrt{2}}(|d_{x^2-y^2}\rangle + i\tau|d_{xy}\rangle), \qquad (1)$$

$\tau = 1(-1)$ for *K(K')*-valley To first order in k, the C_{3h} symmetry dictates that the two-band $k \cdot p$ Hamiltonian has the form

$$\hat{H}_0 = at(\tau k_x\hat{\sigma}_x + k_y\hat{\sigma}_y) + \frac{\Delta}{2}\hat{\sigma}_z, \qquad (2)$$

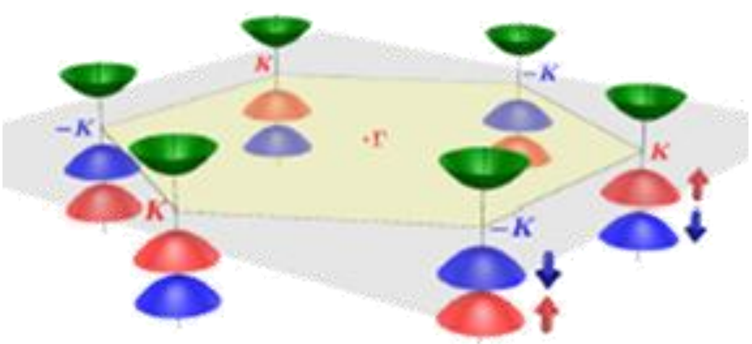

$\vec{k}\cdot\vec{p}$-method in action: Low-energy effective H

- **2D Transition Metal Dichalcogenides**

  → PRL **108**, 196802 (2012)

Counting Symmetry

e.g., Time-reversal symmetry

Now you see $\hat{\Theta} = i\hat{s}_y K$ is correct, $\hat{s}$'s are about spins. Check

$$\hat{\Theta}^{-1}\hat{H}^{\tau}\hat{\Theta} = \hat{s}_y\left[\hat{H}_0^{\tau} - \lambda\tau\frac{\hat{\sigma}_z - 1}{2}\hat{s}_z\right]^{*}\hat{s}_y$$

$$= \hat{H}_0^{-\tau} + \hat{s}_y\left(-\lambda\tau\frac{\hat{\sigma}_z - 1}{2}\hat{s}_z\right)\hat{s}_y$$

$$= \hat{H}_0^{-\tau} - \lambda(-\tau)\frac{\hat{\sigma}_z - 1}{2}\hat{s}_z = \hat{H}^{-\tau}$$

Time-reversal of low-energy H of *K*-valley is that of *K'*-valley

shown in Fig. 1(c). The group of the wave vector at the band edges (K) is C_{3h} and the symmetry adapted basis functions are

$$|\phi_c\rangle = |d_{z^2}\rangle, \qquad |\phi_v^{\tau}\rangle = \frac{1}{\sqrt{2}}(|d_{x^2-y^2}\rangle + i\tau|d_{xy}\rangle), \quad (1)$$

$\tau = 1(-1)$ for *K(K')*-valley

To first order in k, the C_{3h} symmetry dictates that the two-band $k\cdot p$ Hamiltonian has the form

$$\hat{H}_0 = at(\tau k_x\hat{\sigma}_x + k_y\hat{\sigma}_y) + \frac{\Delta}{2}\hat{\sigma}_z, \quad (2)$$

state splits. Approximating the SOC by the intra-atomic contribution $\boldsymbol{L}\cdot\boldsymbol{S}$, we find the total Hamiltonian given by

$$\hat{H} = at(\tau k_x\hat{\sigma}_x + k_y\hat{\sigma}_y) + \frac{\Delta}{2}\hat{\sigma}_z - \lambda\tau\frac{\hat{\sigma}_z - 1}{2}\hat{s}_z, \quad (3)$$

where 2λ is the spin splitting at the valence band top caused by the SOC and $\hat{s}_z$ is the Pauli matrix for spin.

$\vec{k} \cdot \vec{p}$-method in action: Low-energy effective H

- **Graphene: 2nd order perturbation theory**

Intrinsic and Rashba spin-orbit interactions in graphene sheet

→ PRB **74**, 165310 (2006); Mesoscopic interactions are

$$\hat{V} = \hat{H}_{SO} + \hat{H}_{EF} = \frac{1}{2(m_e c)^2}(\nabla \times \vec{p}) \cdot \vec{S} + eE\sum_i z_i$$

i is the lattice site index

→ The 1st order perturbation in $\vec{k} \cdot \vec{p}$-method vanishes

→ The 2nd degenerate state perturbation

Leonard I. Schiff, *Quantum Mechanics*, McGraw-Hill, New York, (1968)

$$H_{m,n}^{(2)} = \sum_{l \notin D} \frac{\langle m^{(0)}|V|l^{(0)}\rangle\langle l^{(0)}|V|n^{(0)}\rangle}{E_E - E_l^{(0)}}$$

→ Low-energy sector

$$= \begin{Bmatrix} |K, p_z A, \uparrow\rangle, |K, p_z A, \downarrow\rangle, |K', p_z A, \uparrow\rangle, |K', p_z A, \downarrow\rangle, \\ |K, p_z B, \uparrow\rangle, |K, p_z B, \downarrow\rangle, |K', p_z B, \uparrow\rangle, |K', p_z B, \downarrow\rangle \end{Bmatrix}$$

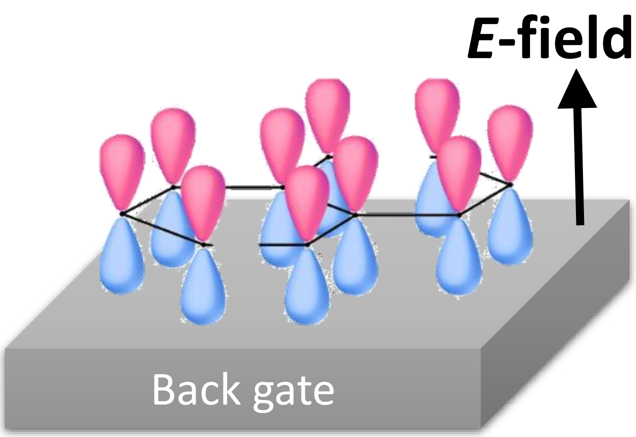

$\vec{k} \cdot \vec{p}$-method in action: Low-energy effective H

- **Graphene: 2nd order perturbation theory**

Intrinsic and Rashba spin-orbit interactions in graphene sheet

→ PRB **74**, 165310 (2006); Mesoscopic interactions are

$$\hat{V} = \hat{H}_{SO} + \hat{H}_{EF} = \frac{1}{2(m_e c)^2}(\nabla \times \vec{p}) \cdot \vec{S} + eE \sum_i z_i$$

i is the lattice site index

→ The 1st order perturbation in $\vec{k} \cdot \vec{p}$-method vanishes

→ The 2nd degenerate state perturbation

$$H_{m,n}^{(2)} = \sum_{l \notin D} \frac{\langle m^{(0)}|V|l^{(0)}\rangle\langle l^{(0)}|V|n^{(0)}\rangle}{E_E - E_l^{(0)}}$$

→ Low-energy sector

$$= \begin{Bmatrix} |K, p_z A, \uparrow\rangle, |K, p_z A, \downarrow\rangle, |K', p_z A, \uparrow\rangle, |K', p_z A, \downarrow\rangle, \\ |K, p_z B, \uparrow\rangle, |K, p_z B, \downarrow\rangle, |K', p_z B, \uparrow\rangle, |K', p_z B, \downarrow\rangle \end{Bmatrix}$$

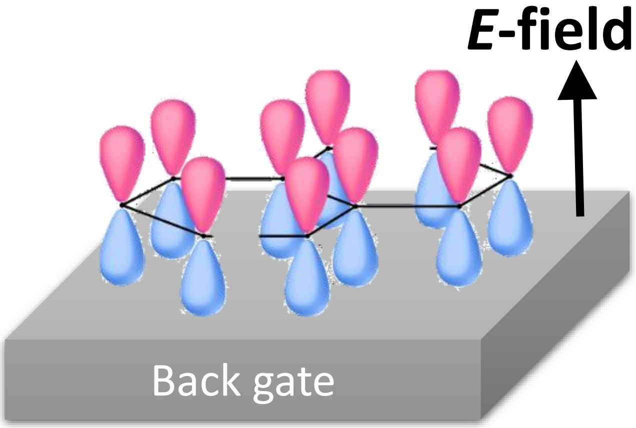

$\vec{k} \cdot \vec{p}$-method in action: Low-energy effective H

- **Graphene: 2nd order perturbation theory**

Intrinsic and Rashba spin-orbit interactions in graphene sheet

→ PRB **74**, 165310 (2006); Mesoscopic interactions are

$$\hat{V} = \hat{H}_{SO} + \hat{H}_{EF} = \frac{1}{2(m_e c)^2}(\nabla \times \vec{p}) \cdot \vec{S} + eE\sum_i z_i$$

i is the lattice site index

→ The 2nd degenerate state perturbation

$$H_{\text{eff}} = -\lambda_{SO} + \lambda_{SO}\sigma_z\tau_z s_z + \lambda_R\left(\sigma_x\tau_z s_y - \sigma_z s_x\right)$$

→ Dirac point at K(K')-valley opens a gap $E_g = 2(\lambda_{SO} - \lambda_R)$

→ $2\lambda_{SO} = \frac{|s|}{9(sp\sigma)^2}\xi^2 \approx 0.00114\ \text{meV} \approx k_B \times 0.0132\ \text{K}$

→ $\lambda_R = \frac{eEz_0}{3(sp\sigma)}\xi \propto E$

Mesoscopic interactions depend on the shape of wavefunctions at low-energy

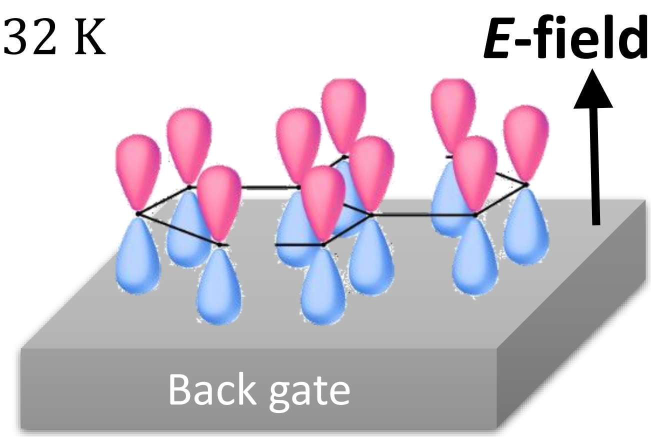

$\vec{k} \cdot \vec{p}$-method in action: Low-energy effective H

- **Graphene as 2D Topological Insulator (TI)**
  - → PRL **95**, 226801 (2005); Quantum Spin Hall Effect in Graphene
  - → PRL **95**, 146802 (2005); Z2 Topological Order and the Quantum Spin Hall Effect
  - → Basically, 2D TIs realize the effective H of graphene

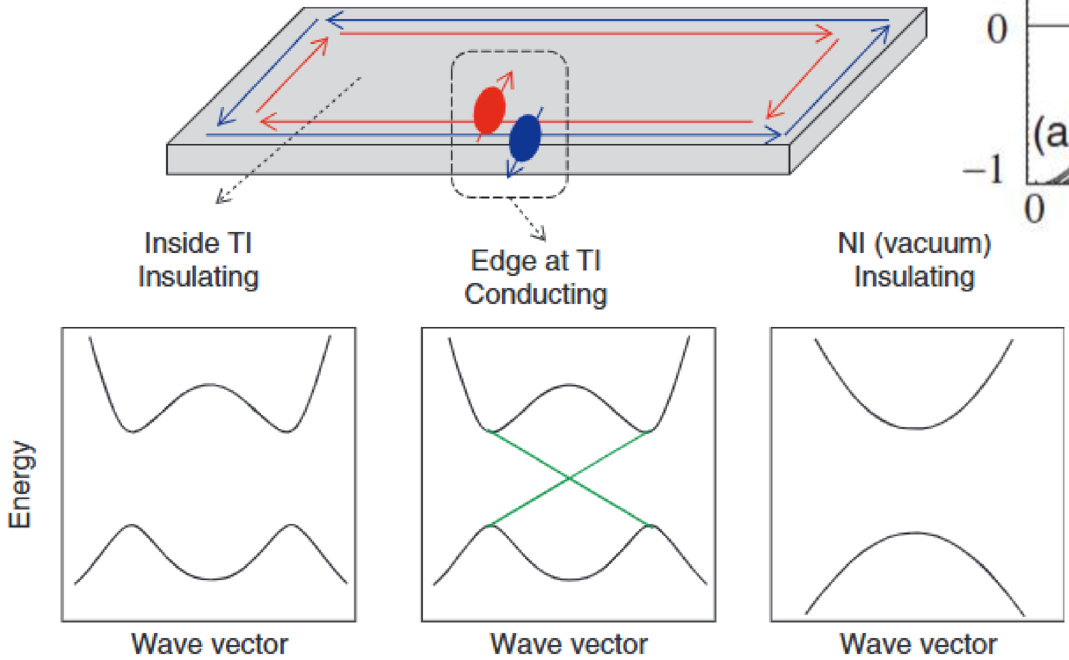

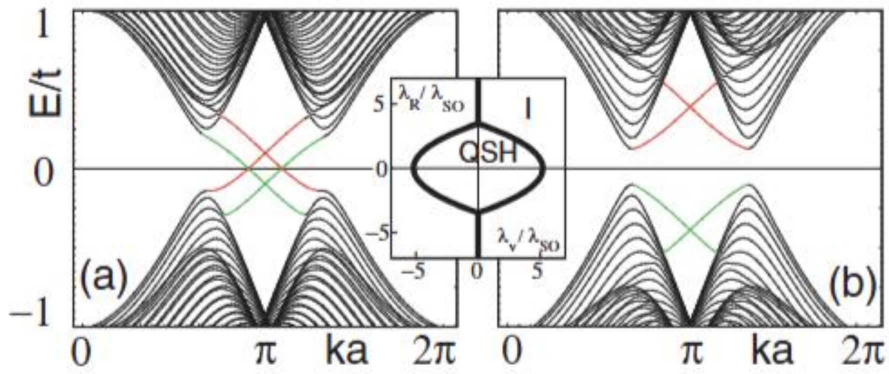

$$\lambda_{SO} \approx k_B \times 0.0066 \text{ K}$$
$$\lambda_R \approx k_B \times 0.129 \text{ K}$$
$$\lambda_R / \lambda_{SO} \approx 20$$

What is Mesoscopic Quantum Transport

- **Low-energy effective Hamiltonian:** $\vec{k} \cdot \vec{p}$-method

  → 1D InAs Nanowire?

p_x →

  → Nano Letters 16, 5135 (2016)

Direct Measurements of Fermi Level Pinning at the Surface of Intrinsically n-Type InGaAs Nanowires

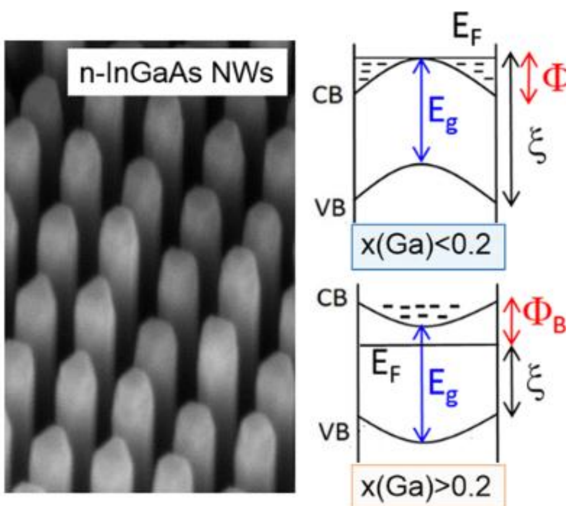

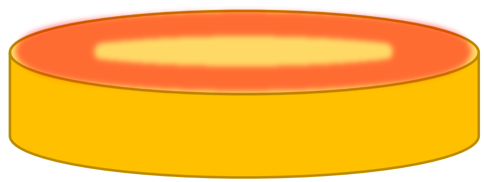

Select low-energy sector with $|p_x = 0, \uparrow\rangle$ & $|p_x = 0, \downarrow\rangle$

$$H_{\text{eff}}(p_x) = \begin{pmatrix} \langle 0, \uparrow | \hat{H}(p_x) | 0, \uparrow \rangle & \langle 0, \uparrow | \hat{H}(p_x) | 0, \downarrow \rangle \\ \langle 0, \downarrow | \hat{H}(p_x) | 0, \uparrow \rangle & \langle 0, \downarrow | \hat{H}(p_x) | 0, \downarrow \rangle \end{pmatrix}$$

What is Mesoscopic Quantum Transport

- **Low-energy effective Hamiltonian:** $\vec{k} \cdot \vec{p}$-method

→ 1D InAs Nanowire?

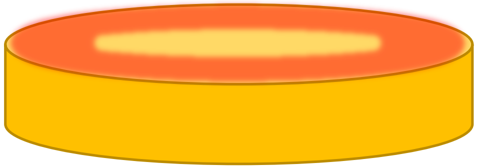

Select low-energy sector with $|p_x = 0, \uparrow\rangle$ & $|p_x = 0, \downarrow\rangle$

$$H_{\mathrm{eff}}(p_x) = \begin{pmatrix} \langle 0, \uparrow | \hat{H}(p_x) | 0, \uparrow \rangle & \langle 0, \uparrow | \hat{H}(p_x) | 0, \downarrow \rangle \\ \langle 0, \downarrow | \hat{H}(p_x) | 0, \uparrow \rangle & \langle 0, \downarrow | \hat{H}(p_x) | 0, \downarrow \rangle \end{pmatrix}$$

- **Mesoscopic Interaction ≠ interaction w/ bare electrons**

→ Very high Landé g-factor, $g \approx 14$ ($g \approx 2$ for bare electrons)

$$H_Z = -\vec{\mu} \cdot \vec{B} = g\mu_B \vec{S} \cdot \vec{B}$$

→ Tunable Landé g-factor: PRB **72**, 201307(R) (2005)

→ Tunable Spin-orbit interaction: Nanoscale Adv. **4**, 2642 (2022)

MQT in action: $\frac{dI}{dV}$ of topological system from S-matrix

- **Reproducing journal papers: Quantum Transport in TSC**

  → PRL **102**, 216403 (2009), PRL **102**, 216404 (2009), and PRL **103**, 237001 (2009)

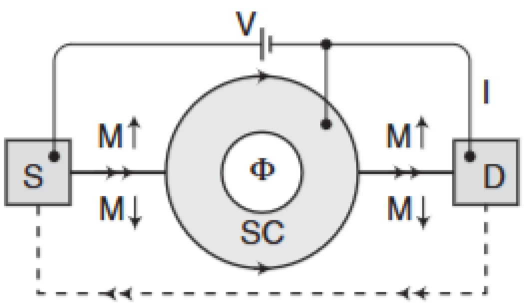

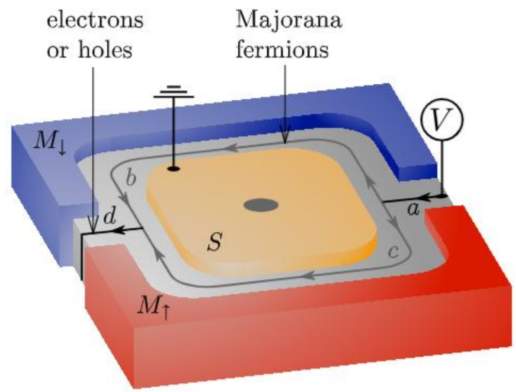

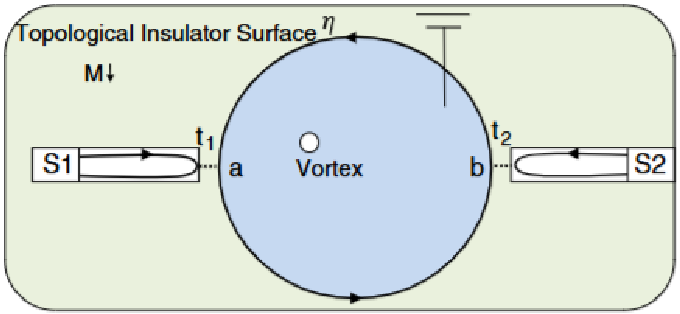

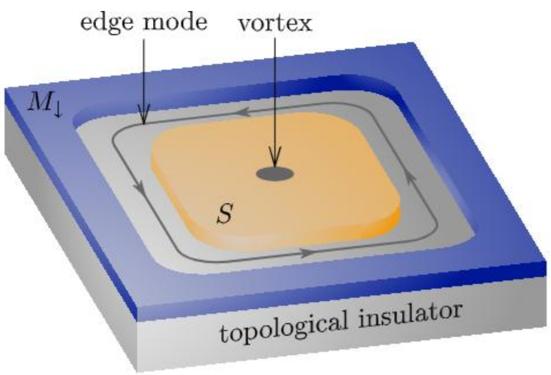

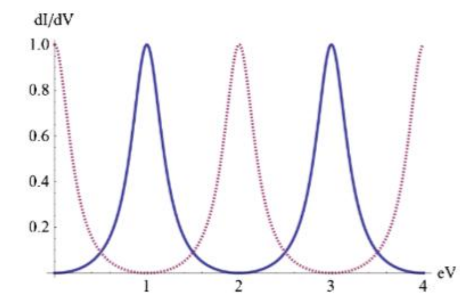

FIG. 3 (color online). dI/dV vs eV with $\tilde{t}_1^4 = 0.1$. eV is in units of $\pi\hbar v_m/L$ and dI/dV is in units of $\frac{2e^2}{h}$. Solid (dashed) line represents the case with even (odd) number of vortices in the superconductor.

MQT in action: $\frac{dI}{dV}$ of topological system from S-matrix

- **Quantum Transport in TSC**

  → Majorana zero modes (MZM) always come in pair

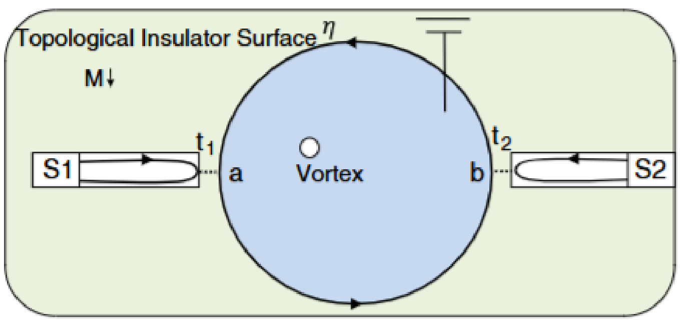

Conductance quantum, as MZM = equal superposition of electron & hole

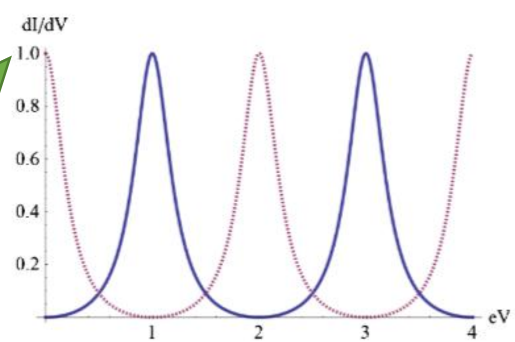

FIG. 3 (color online). dI/dV vs eV with $\tilde{t}_1^4 = 0.1$. eV is in units of $\pi\hbar v_m/L$ and dI/dV is in units of $\frac{2e^2}{h}$. Solid (dashed) line represents the case with even (odd) number of vortices in the superconductor.

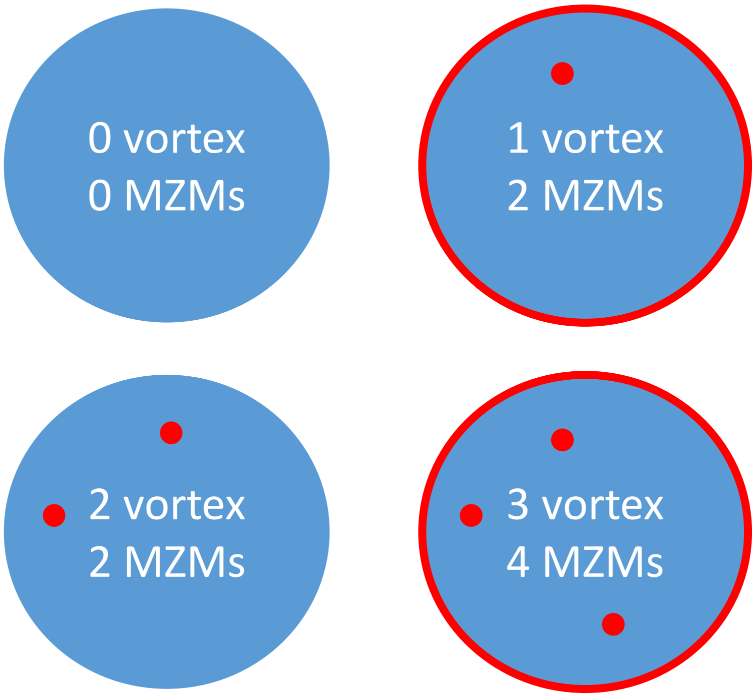

Quantization condition along BC

$$kL + \pi + n_v\pi = 2m\pi,$$

where n_v is # of vortices.

MQT in action: $\frac{dI}{dV}$ of topological system from S-matrix

PRL **102,** 216404 (2009) PHYSICAL REVIEW LETTERS week ending 29 MAY 2009

Electrically Detected Interferometry of Majorana Fermions in a Topological Insulator

A. R. Akhmerov, Johan Nilsson, and C. W. J. Beenakker

Instituut-Lorentz, Universiteit Leiden, P.O. Box 9506, 2300 RA Leiden, The Netherlands

(Received 16 March 2009; published 28 May 2009)

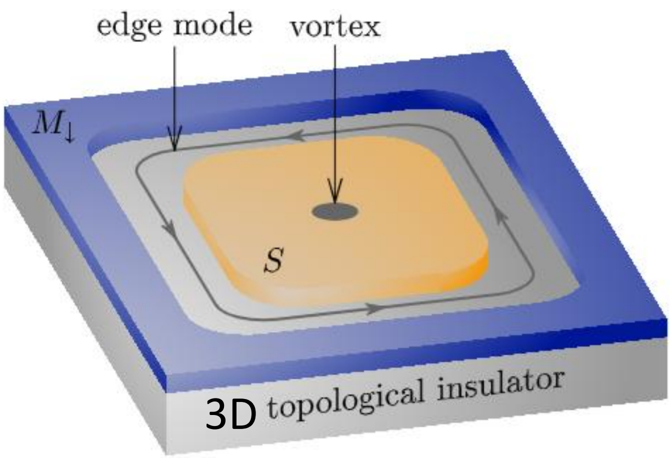

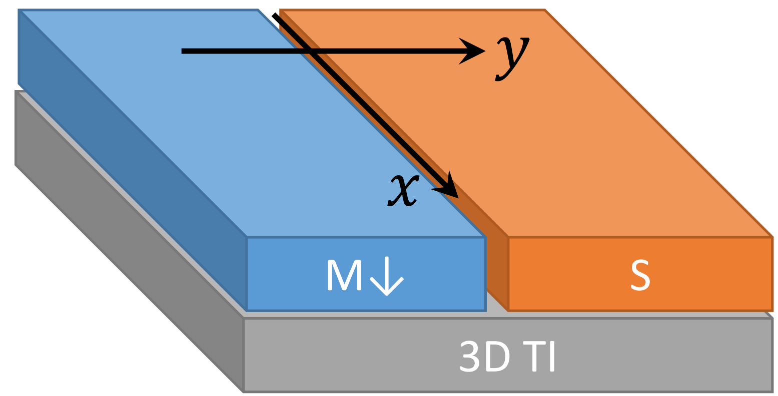

$$H = \begin{pmatrix} \boldsymbol{M}\cdot\boldsymbol{\sigma} + v_F\boldsymbol{p}\cdot\boldsymbol{\sigma} - E_F & \Delta \\ \Delta^* & \boldsymbol{M}\cdot\boldsymbol{\sigma} - v_F\boldsymbol{p}\cdot\boldsymbol{\sigma} + E_F \end{pmatrix}. \quad (3)$$

$\vec{k}\cdot\vec{p}$-method, around $k_x = 0$

$$M(x,y) = \begin{cases} -M, & y < 0 \\ 0, & y > 0 \end{cases}$$

$$\Delta(x,y) = \begin{cases} 0, & y < 0 \\ \Delta e^{i\varphi(x,y)}, & y > 0 \end{cases}$$

MQT in action: $\frac{dI}{dV}$ of topological system from S-matrix

- **Low-energy Hamiltonian**

$$H = \begin{pmatrix} \boldsymbol{M}\cdot\boldsymbol{\sigma} + v_F \boldsymbol{p}\cdot\boldsymbol{\sigma} - E_F & \Delta \\ \Delta^* & \boldsymbol{M}\cdot\boldsymbol{\sigma} - v_F \boldsymbol{p}\cdot\boldsymbol{\sigma} + E_F \end{pmatrix}. \quad (3)$$

$H(p_x = 0)$

$$= \begin{pmatrix} -M\sigma_z - i\hbar v_F \partial_y \sigma_y & 0 \\ 0 & -M\sigma_z + i\hbar v_F \partial_y \sigma_y \end{pmatrix}\Theta(-y) + \begin{pmatrix} -i\hbar v_F \partial_y \sigma_y & \Delta e^{i\varphi} \\ \Delta e^{-i\varphi} & +i\hbar v_F \partial_y \sigma_y \end{pmatrix}\Theta(y)$$

$$= \begin{pmatrix} -M & -\hbar v_F \partial_y & 0 & 0 \\ \hbar v_F \partial_y & M & 0 & 0 \\ 0 & 0 & -M & \hbar v_F \partial_y \\ 0 & 0 & -\hbar v_F \partial_y & M \end{pmatrix}\Theta(-y) + \begin{pmatrix} 0 & -\hbar v_F \partial_y & \Delta e^{i\varphi} & 0 \\ \hbar v_F \partial_y & 0 & 0 & \Delta e^{i\varphi} \\ \Delta e^{-i\varphi} & 0 & 0 & -\hbar v_F \partial_y \\ 0 & \Delta e^{-i\varphi} & \hbar v_F \partial_y & 0 \end{pmatrix}\Theta(y)$$

Zero-energy solutions

Region: $y < 0$

$$\psi(y) \propto e^{\frac{M}{\hbar v_F} y}\left[A\begin{pmatrix}1\\-1\\0\\0\end{pmatrix} + B\begin{pmatrix}0\\0\\1\\1\end{pmatrix}\right]$$

Region: $y > 0$

$$\psi(y) \propto e^{-\frac{\Delta}{\hbar v_F} y}\left[C\begin{pmatrix}e^{\frac{i\varphi}{2}}\\0\\0\\e^{-\frac{i\varphi}{2}}\end{pmatrix} + D\begin{pmatrix}0\\e^{\frac{i\varphi}{2}}\\-e^{-\frac{i\varphi}{2}}\\0\end{pmatrix}\right]$$

MQT in action: $\frac{dI}{dV}$ of topological system from S-matrix

- **Wave function matching at y=0**

$$A\begin{pmatrix}1\\-1\\0\\0\end{pmatrix}+B\begin{pmatrix}0\\0\\1\\1\end{pmatrix}=C\begin{pmatrix}e^{\frac{i\varphi}{2}}\\0\\0\\e^{-\frac{i\varphi}{2}}\end{pmatrix}+D\begin{pmatrix}0\\e^{\frac{i\varphi}{2}}\\-e^{-\frac{i\varphi}{2}}\\0\end{pmatrix}\Leftrightarrow\begin{pmatrix}0\\0\\0\\0\end{pmatrix}=\overbrace{\begin{pmatrix}1&0&-e^{\frac{i\varphi}{2}}&0\\-1&0&0&-e^{\frac{i\varphi}{2}}\\0&1&0&e^{-\frac{i\varphi}{2}}\\0&1&-e^{-\frac{i\varphi}{2}}&0\end{pmatrix}}^{\tilde{Q}}\begin{pmatrix}A\\B\\C\\D\end{pmatrix}$$

$\det\tilde{Q}=0\Leftrightarrow$ There exists the topological zero-energy state.

$$A=-e^{\frac{i\varphi}{2}},B=-e^{-\frac{i\varphi}{2}},C=-1,D=1$$

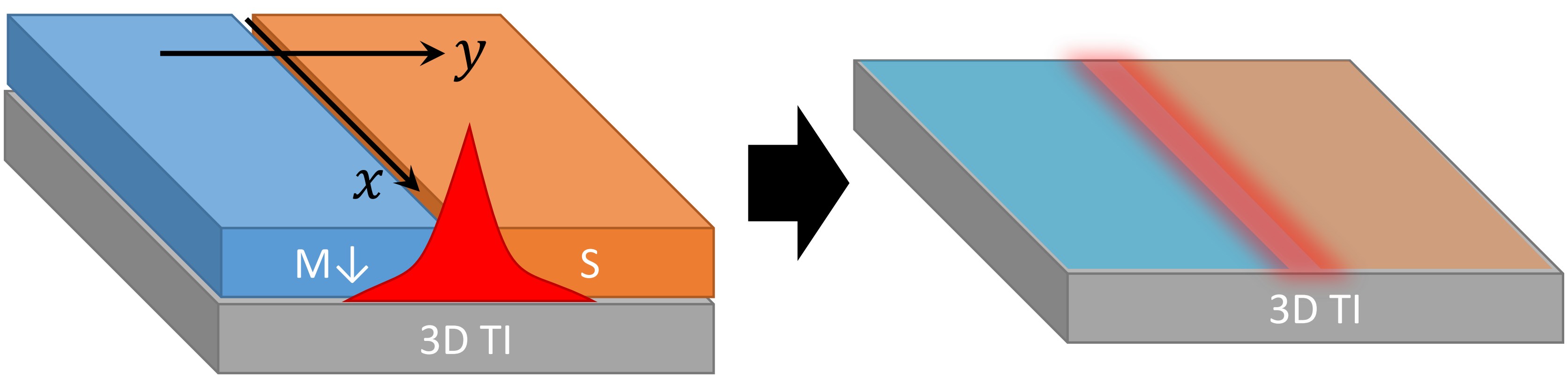

MQT in action: $\frac{dI}{dV}$ of topological system from S-matrix

- **Wave function matching at y=0**

$$A\begin{pmatrix}1\\-1\\0\\0\end{pmatrix}+B\begin{pmatrix}0\\0\\1\\1\end{pmatrix}=C\begin{pmatrix}e^{\frac{i\varphi}{2}}\\0\\0\\e^{-\frac{i\varphi}{2}}\end{pmatrix}+D\begin{pmatrix}0\\e^{\frac{i\varphi}{2}}\\-e^{-\frac{i\varphi}{2}}\\0\end{pmatrix}\Leftrightarrow\begin{pmatrix}0\\0\\0\\0\end{pmatrix}=\overbrace{\begin{pmatrix}1&0&-e^{\frac{i\varphi}{2}}&0\\-1&0&0&-e^{\frac{i\varphi}{2}}\\0&1&0&e^{-\frac{i\varphi}{2}}\\0&1&-e^{-\frac{i\varphi}{2}}&0\end{pmatrix}}^{\tilde{Q}}\begin{pmatrix}A\\B\\C\\D\end{pmatrix}$$

$\det\tilde{Q}=0\Leftrightarrow$ There exists the topological zero-energy state.

$$A=e^{\frac{i\varphi}{2}},B=e^{-\frac{i\varphi}{2}},C=1,D=-1$$

If $M=\Delta$, analytical expression is simple

$$\psi(y)\propto e^{-\frac{\Delta}{\hbar v_F}|y|}\begin{pmatrix}e^{\frac{i\varphi}{2}}\\-e^{\frac{i\varphi}{2}}\\e^{-\frac{i\varphi}{2}}\\e^{-\frac{i\varphi}{2}}\end{pmatrix}$$

Particle-hole symmetry is expressed by the anticommutation $H\Xi=-\Xi H$ of the Hamiltonian with the operator

$$\Xi=\begin{pmatrix}0&i\sigma_y\mathcal{C}\\-i\sigma_y\mathcal{C}&0\end{pmatrix}, \qquad (4)$$

Try checking $\Xi\psi(y)=\psi(y)$: Majorana mode

MQT in action: $\frac{dI}{dV}$ of topological system from S-matrix

- **Low-energy Hamiltonian: chiral Majorana mode**

$$H_{\text{eff}}(p_x) = \int_{-\infty}^{\infty} \psi^+(y) H(p_x, -i\hbar\partial_y)\psi(y)dy \propto \hbar v_F p_x$$

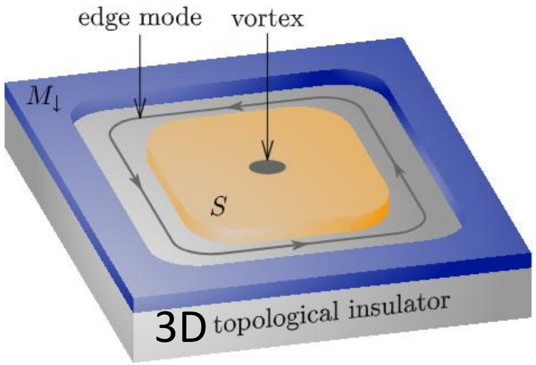

- **Recall basis of the chiral Majorana mode**

$$\psi(y) \propto e^{-\frac{\Delta}{\hbar v_F}|y|} \begin{pmatrix} e^{\frac{i\varphi}{2}} \\ -e^{\frac{i\varphi}{2}} \\ e^{-\frac{i\varphi}{2}} \\ e^{-\frac{i\varphi}{2}} \end{pmatrix}, \text{ where } \varphi = \varphi(\vec{r}) \text{ and } \vec{r} \in S$$

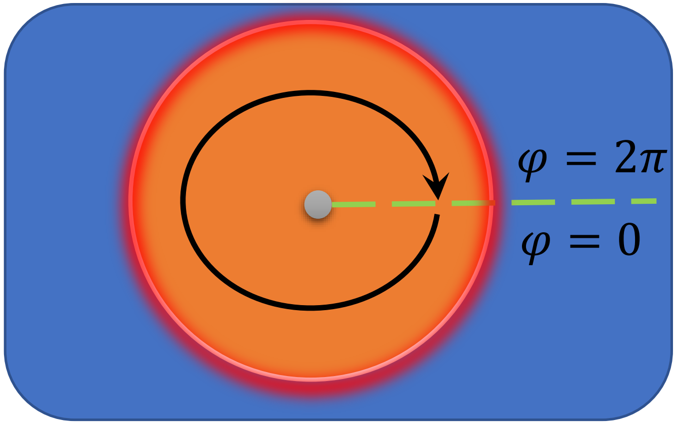

For $\varphi \mapsto \varphi + 2\pi$, $\psi(y)$ accumulates π-phase

$$\text{For } \varphi \mapsto \varphi + 2\pi, \begin{pmatrix} e^{\frac{i\varphi}{2}} \\ -e^{\frac{i\varphi}{2}} \\ e^{-\frac{i\varphi}{2}} \\ e^{-\frac{i\varphi}{2}} \end{pmatrix} \mapsto - \begin{pmatrix} e^{\frac{i\varphi}{2}} \\ -e^{\frac{i\varphi}{2}} \\ e^{-\frac{i\varphi}{2}} \\ e^{-\frac{i\varphi}{2}} \end{pmatrix}$$

MQT in action: $\frac{dI}{dV}$ of topological system from S-matrix

- **Low-energy Hamiltonian: chiral Majorana mode**

$$H_{\text{eff}}(p_x) = \int_{-\infty}^{\infty} \psi^{+}(y) H\left(p_x, -i\hbar\partial_y\right)\psi(y)dy \propto \hbar v_F p_x$$

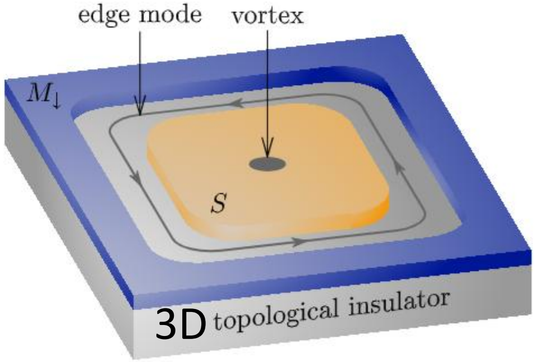

- **The quantization condition:**

as $\psi(y)$ accumulates π-phase For $\varphi \mapsto \varphi + 2\pi$,

$$kL + \pi + n_v\pi = 2m\pi$$

Berry phase

Below spinor rotates along boundary

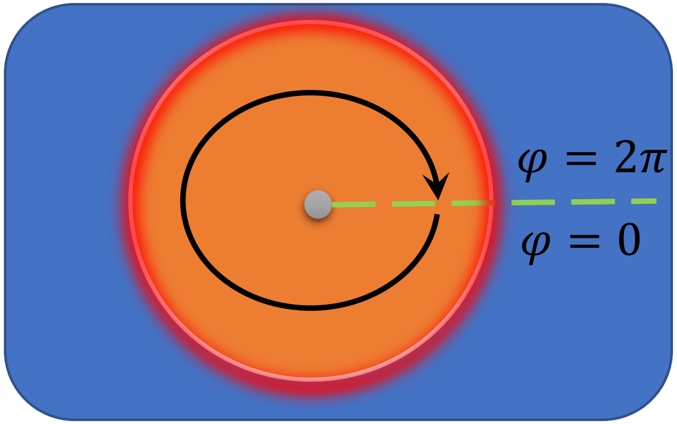

$$\psi(y) \propto e^{-\frac{\Delta}{\hbar v_F}|y|}\begin{pmatrix} e^{\frac{i\varphi}{2}} \\ -e^{\frac{i\varphi}{2}} \\ e^{-\frac{i\varphi}{2}} \\ e^{-\frac{i\varphi}{2}} \end{pmatrix}$$

MQT in action: $\frac{dI}{dV}$ of topological system from S-matrix

- **Low-energy Hamiltonian: chiral Majorana mode**

$$H_{\mathrm{eff}}(p_x) = \int_{-\infty}^{\infty} \psi^+(y) H\left(p_x, -i\hbar\partial_y\right)\psi(y)\,dy \propto \hbar v_F p_x$$

- **The quantization condition:**

$$kL + \pi + n_v\pi = 2m\pi$$

- **Quantized Energies**

$$E_m = \hbar v_F k_m$$

$$= (2m - 1 - n_v)\boxed{\frac{\pi\hbar v_F}{L}}$$

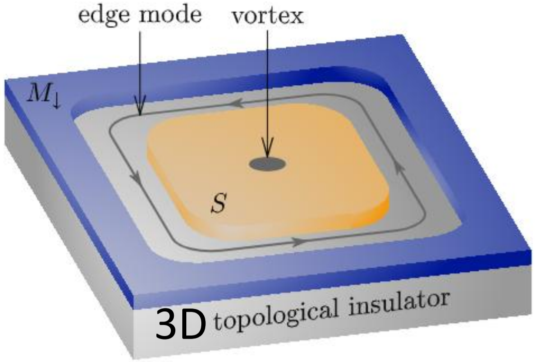

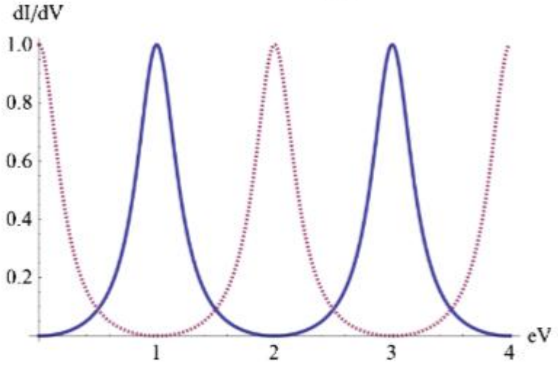

FIG. 3 (color online). dI/dV vs eV with $\tilde{t}_1^4 = 0.1$. eV is in units of $\boxed{\pi\hbar v_m/L}$ and dI/dV is in units of $\frac{2e^2}{h}$. Solid (dashed) line represents the case with even (odd) number of vortices in the superconductor.

MQT in action: $\frac{dI}{dV}$ of topological system from S-matrix

- **Low-energy Hamiltonian: chiral Majorana mode**

$$H_{\text{eff}}(p_x) = \int_{-\infty}^{\infty} \psi^+(y) H(p_x, -i\hbar\partial_y)\psi(y)dy \propto \hbar v_F p_x$$

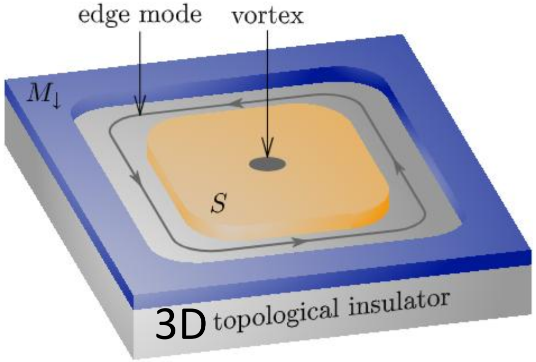

- **The quantization condition:**

$$kL + \pi + n_v\pi = 2m\pi$$

- **Quantized Energies**

$$E_m = \hbar v_F k_m$$

$$= (2m - 1 - n_v)\boxed{\frac{\pi\hbar v_F}{L}}$$

Conductance quantum, as MZM = equal superposition of electron & hole

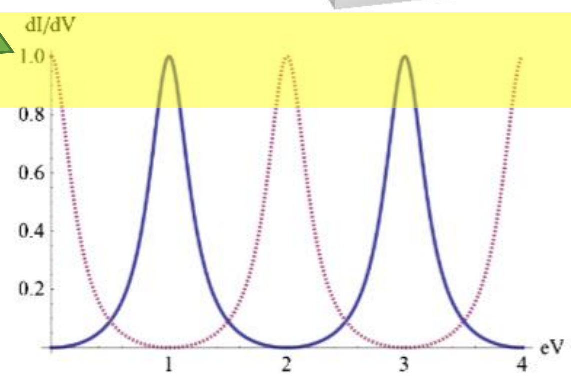

FIG. 3 (color online). dI/dV vs eV with $\tilde{t}_1^4 = 0.1$. eV is in units of $\boxed{\pi\hbar v_m/L}$ and dI/dV is in units of $\frac{2e^2}{h}$. Solid (dashed) line represents the case with even (odd) number of vortices in the superconductor.

MQT in action: $\frac{dI}{dV}$ of topological system from S-matrix

- **Try:** derive the low-energy Hamiltonian of below using $\vec{k} \cdot \vec{p}$-method (it should be chiral electron & hole modes)

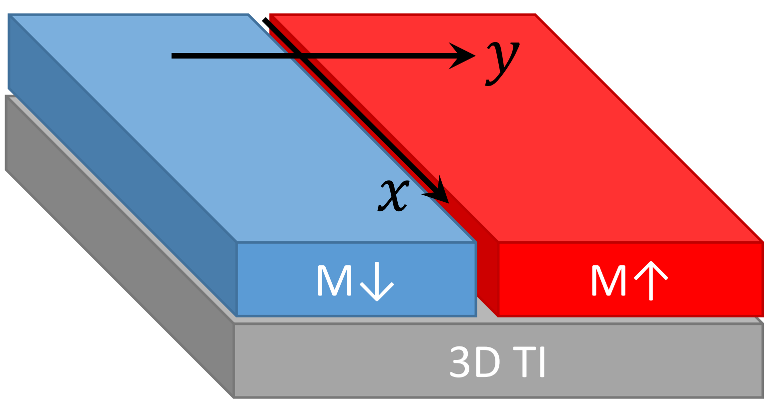

MQT in action: $\frac{dI}{dV}$ of topological system from S-matrix

- **Mesoscopic Quantum Transport in TSC using S-matrix**

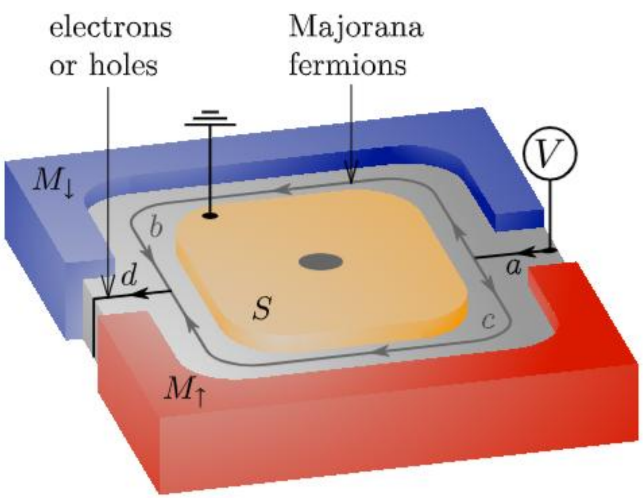

=

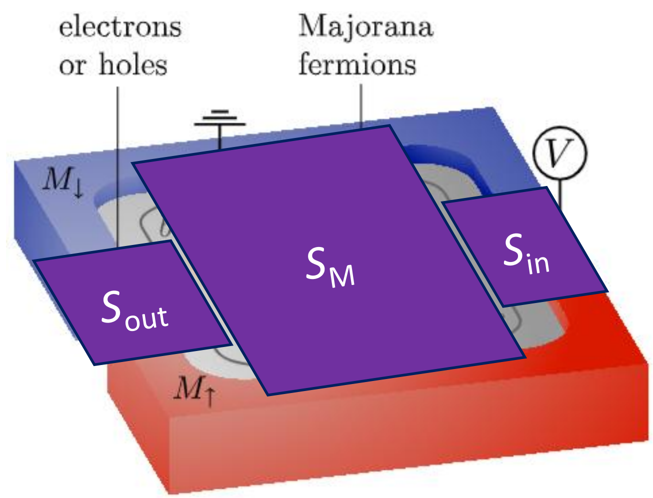

=

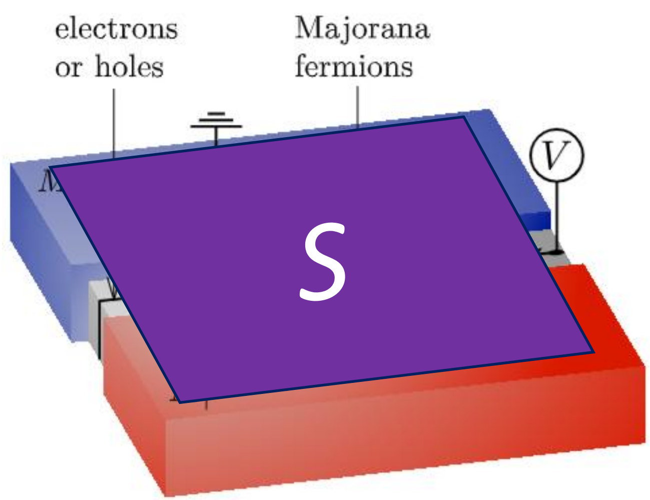

$$\boxed{I = \frac{2e}{h} \int_0^{eV} T(E)dE}$$

MQT in action: $\frac{dI}{dV}$ of topological system from S-matrix

- **Symmetry of S_{in}-matrix: particle-hole**

$$\begin{pmatrix} \psi_b \\ \psi_c \end{pmatrix} = S_{\text{in}} \begin{pmatrix} \phi_a^e \\ \phi_a^h \end{pmatrix}. \tag{5}$$

Particle-hole symmetry for the scattering matrix is expressed by

$$S_{\text{in}}(\varepsilon) = S_{\text{in}}^*(-\varepsilon) \begin{pmatrix} 0 & 1 \\ 1 & 0 \end{pmatrix}. \tag{6}$$

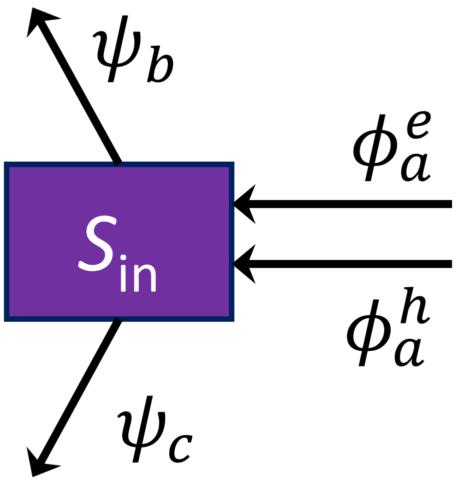

$\rightarrow \left|\Psi_{in}^E\right\rangle = \phi_a^e|\phi_a^e\rangle + \phi_a^h|\phi_a^h\rangle$ is an incoming state at energy E.

i.e., $\hat{H}|\Psi_N\rangle = E|\Psi_N\rangle$ with $\hat{H}\left(\hat{\Xi}|\Psi_N\rangle\right) = -\hat{\Xi}\hat{H}\hat{\Xi}^{-1}\left(\hat{\Xi}|\Psi_N\rangle\right) = -E\left(\hat{\Xi}|\Psi_N\rangle\right)$

$\therefore \hat{\Xi}|\Psi_N\rangle$ is the energy eigenstate of $-E$ and it's an incoming state.

c.f., $\hat{\Xi}|\Psi_N\rangle = \hat{\Xi}\left(\phi_a^e|\phi_a^e\rangle + \phi_a^h\left|\phi_a^h\right\rangle\right) = \left(\phi_a^h\right)^*|\phi_a^e\rangle + (\phi_a^e)^*\left|\phi_a^h\right\rangle$

$\therefore$ given incoming $\begin{pmatrix} \phi_a^e \\ \phi_a^h \end{pmatrix}$ at E, incoming at $-E$ is known $\begin{pmatrix} \left(\phi_a^h\right)^* \\ (\phi_a^e)^* \end{pmatrix}$

MQT in action: $\frac{dI}{dV}$ of topological system from S-matrix

- **Symmetry of S_{in}-matrix: particle-hole**

$$\begin{pmatrix} \psi_b \\ \psi_c \end{pmatrix} = S_{\text{in}} \begin{pmatrix} \phi_a^e \\ \phi_a^h \end{pmatrix}. \quad (5)$$

Particle-hole symmetry for the scattering matrix is expressed by

$$S_{\text{in}}(\varepsilon) = S_{\text{in}}^*(-\varepsilon) \begin{pmatrix} 0 & 1 \\ 1 & 0 \end{pmatrix}. \quad (6)$$

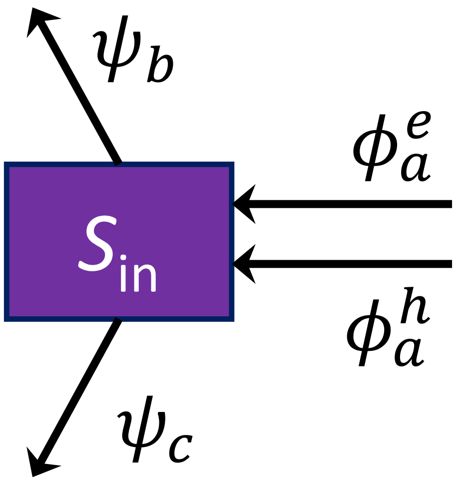

$\rightarrow |\Psi_{\text{in}}^E\rangle = \phi_a^e|\phi_a^e\rangle + \phi_a^h|\phi_a^h\rangle$ is an incoming state at energy E.

i.e., $\hat{H}|\Psi_{\text{in}}^E\rangle = E|\Psi_{\text{in}}^E\rangle$ with $\hat{H}\left(\hat{\Xi}|\Psi_{\text{in}}^E\rangle\right) = -\hat{\Xi}\hat{H}\hat{\Xi}^{-1}\left(\hat{\Xi}|\Psi_{\text{in}}^E\rangle\right) = -E\left(\hat{\Xi}|\Psi_{\text{in}}^E\rangle\right)$

$\therefore \hat{\Xi}|\Psi_{\text{in}}^E\rangle$ is the energy eigenstate of $-E$ and it's an incoming state.

c.f., $|\Psi_{\text{in}}^{-E}\rangle = \hat{\Xi}\left(\phi_a^e|\phi_a^e\rangle + \phi_a^h|\phi_a^h\rangle\right) = \left(\phi_a^h\right)^*|\phi_a^e\rangle + \left(\phi_a^e\right)^*|\phi_a^h\rangle$

$\therefore$ **given incoming** $\begin{pmatrix} \phi_a^e \\ \phi_a^h \end{pmatrix}$ **at** E**, incoming at** $-E$ **is known** $\begin{pmatrix} \left(\phi_a^h\right)^* \\ \left(\phi_a^e\right)^* \end{pmatrix}$

MQT in action: $\frac{dI}{dV}$ of topological system from S-matrix

- **Symmetry of S_{in}-matrix: particle-hole**

$$\begin{pmatrix} \psi_b \\ \psi_c \end{pmatrix} = S_{\text{in}} \begin{pmatrix} \phi_a^e \\ \phi_a^h \end{pmatrix}. \tag{5}$$

Particle-hole symmetry for the scattering matrix is expressed by

$$S_{\text{in}}(\varepsilon) = S_{\text{in}}^{*}(-\varepsilon) \begin{pmatrix} 0 & 1 \\ 1 & 0 \end{pmatrix}. \tag{6}$$

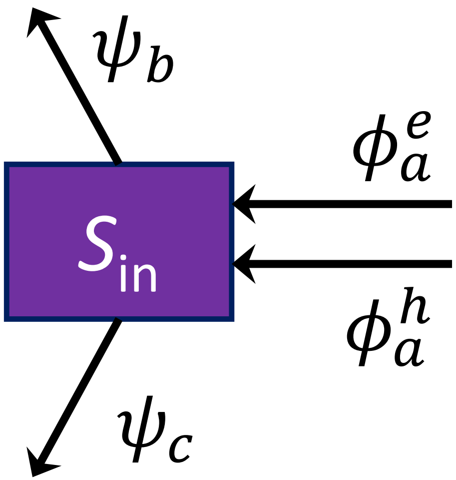

$\rightarrow |\Psi_{b,c}^{E}\rangle = \psi_{b,c}|\psi_{b,c}\rangle$ is an outgoing state.

$\hat{\Xi}|\Psi_{b,c}^{E}\rangle$ is the energy eigenstate of $-E$ and it's an incoming state.

c.f., $|\Psi_{b,c}^{-E}\rangle = \hat{\Xi}(\psi_{b,c}|\psi_{b,c}\rangle) = \psi_{b,c}^{*}|\psi_{b,c}\rangle$

$\therefore$ **given outgoing** $\begin{pmatrix} \psi_b \\ \psi_c \end{pmatrix}$ **at** E**, outgoing at** $-E$ **is known** $\begin{pmatrix} \psi_b^{*} \\ \psi_c^{*} \end{pmatrix}$

MQT in action: $\frac{dI}{dV}$ of topological system from S-matrix

- **Symmetry of S_{in}-matrix: particle-hole**

$$\begin{pmatrix} \psi_b \\ \psi_c \end{pmatrix} = S_{\text{in}} \begin{pmatrix} \phi_a^e \\ \phi_a^h \end{pmatrix}. \tag{5}$$

Particle-hole symmetry for the scattering matrix is expressed by

$$S_{\text{in}}(\varepsilon) = S_{\text{in}}^*(-\varepsilon) \begin{pmatrix} 0 & 1 \\ 1 & 0 \end{pmatrix}. \tag{6}$$

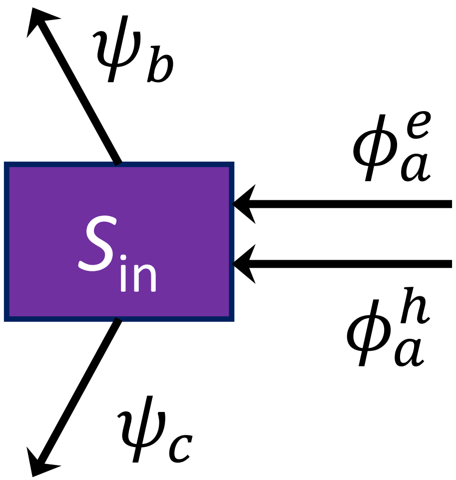

$\rightarrow$ **given incoming** $\begin{pmatrix} \phi_a^e \\ \phi_a^h \end{pmatrix}$ **at** E**, incoming at** $-E$ **is known** $\begin{pmatrix} (\phi_a^h)^* \\ (\phi_a^e)^* \end{pmatrix}$

$\rightarrow$ **given outgoing** $\begin{pmatrix} \psi_b \\ \psi_c \end{pmatrix}$ **at** E**, outgoing at** $-E$ **is known** $\begin{pmatrix} \psi_b^* \\ \psi_c^* \end{pmatrix}$

Hence, $\begin{pmatrix} \psi_b^* \\ \psi_c^* \end{pmatrix} = S_{\text{in}}(-E) \begin{pmatrix} (\phi_a^h)^* \\ (\phi_a^e)^* \end{pmatrix} \Leftrightarrow \begin{pmatrix} \psi_b \\ \psi_c \end{pmatrix} = S_{\text{in}}^*(-E) \begin{pmatrix} 0 & 1 \\ 1 & 0 \end{pmatrix} \begin{pmatrix} \phi_a^e \\ \phi_a^h \end{pmatrix}$

MQT in action: $\frac{dI}{dV}$ of topological system from S-matrix

- **Symmetry of S_{in}-matrix: particle-hole**

At small excitation energies $|\varepsilon| \ll |M_z|, |\Delta|$ the ε dependence of S_{in} may be neglected. (The excitation energy is limited by the largest of voltage V and temperature T.) Then Eq. (6) together with unitarity ($S_{\text{in}}^{-1} = S_{\text{in}}^{\dagger}$) fully determine the scattering matrix,

$$S_{\text{in}} = \frac{1}{\sqrt{2}} \begin{pmatrix} 1 & 1 \\ \pm i & \mp i \end{pmatrix} \begin{pmatrix} e^{i\alpha} & 0 \\ 0 & e^{-i\alpha} \end{pmatrix}, \tag{7}$$

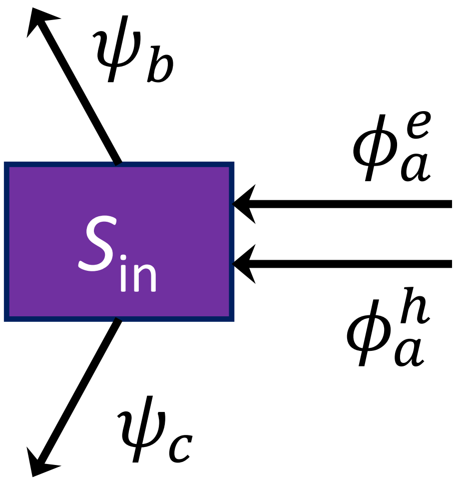

→ $S_{\text{in}} = S_{\text{in}}^* \begin{pmatrix} 0 & 1 \\ 1 & 0 \end{pmatrix}$ and by using unitarity. The sign ambiguity & α is undetermined but does not affect the conductance.

→ **Try!**

MQT in action: $\frac{dI}{dV}$ of topological system from S-matrix

- **Symmetry of S_{out}-matrix: time-reversal**

The scattering matrix S_{out} for the conversion from Majorana modes to electron and hole modes can be obtained from S_{in} by time reversal,

$$S_{\text{out}}(\boldsymbol{M}) = S_{\text{in}}^{T}(-\boldsymbol{M}) = \frac{1}{\sqrt{2}}\begin{pmatrix} e^{i\alpha'} & 0 \\ 0 & e^{-i\alpha'} \end{pmatrix}\begin{pmatrix} 1 & \pm i \\ 1 & \mp i \end{pmatrix}. \quad (8)$$

The phase shift α' may be different from α, because of the sign change of $\boldsymbol{M}$ upon time reversal, but it will also drop out of the conductance.

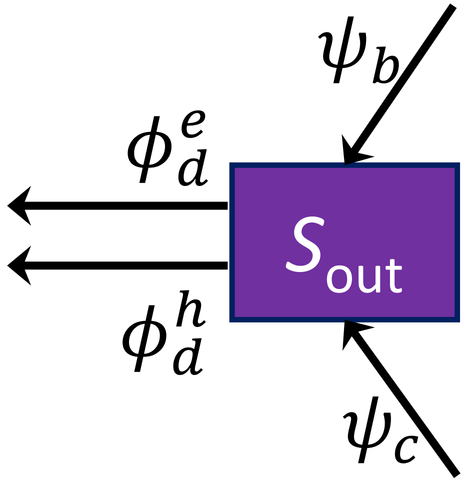

→ Just use time-reversal symmetry!

→ **Try it!** (You've learned how to apply the time-reversal operator to a low-energy Hamiltonian & S-matrix)

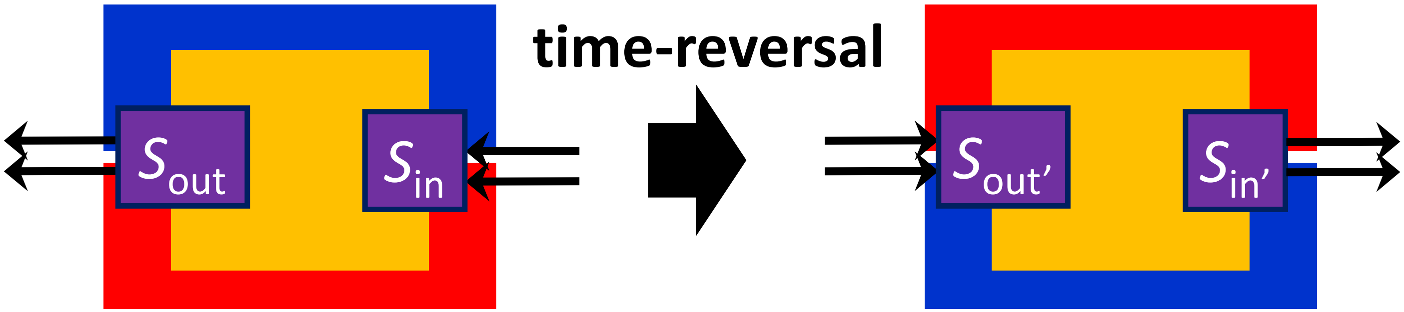

MQT in action: $\frac{dI}{dV}$ of topological system from S-matrix

- **S_M-matrix**

$$\begin{pmatrix}\psi_b\\ \psi_c\end{pmatrix}_{\text{out}} = \begin{pmatrix} e^{i\beta_b} & 0 \\ 0 & e^{i\beta_c}\end{pmatrix}\begin{pmatrix}\psi_b\\ \psi_c\end{pmatrix}_{\text{in}}$$

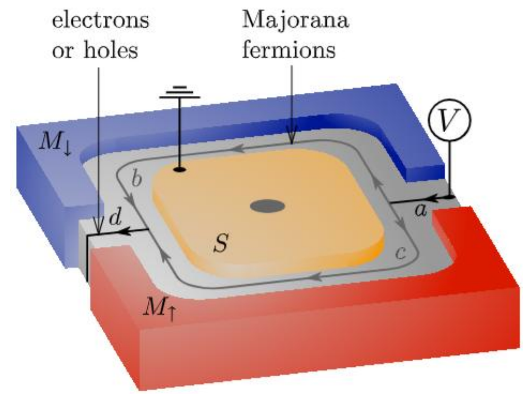

→ Just picking up phases with scattering. But we know

$$\beta_b - \beta_c = kL + \pi + n_v\pi = \frac{EL}{\hbar v_F} + \pi + n_v\pi$$

- **S-matrix**

$$S = \frac{1}{2}\begin{pmatrix} e^{i(\alpha+\alpha')}\left(e^{i\beta_b} - e^{i\beta_c}\right) & e^{-i(\alpha-\alpha')}\left(e^{i\beta_b} + e^{i\beta_c}\right) \\ e^{i(\alpha-\alpha')}\left(e^{i\beta_b} + e^{i\beta_c}\right) & e^{-i(\alpha+\alpha')}\left(e^{i\beta_b} - e^{i\beta_c}\right)\end{pmatrix}$$

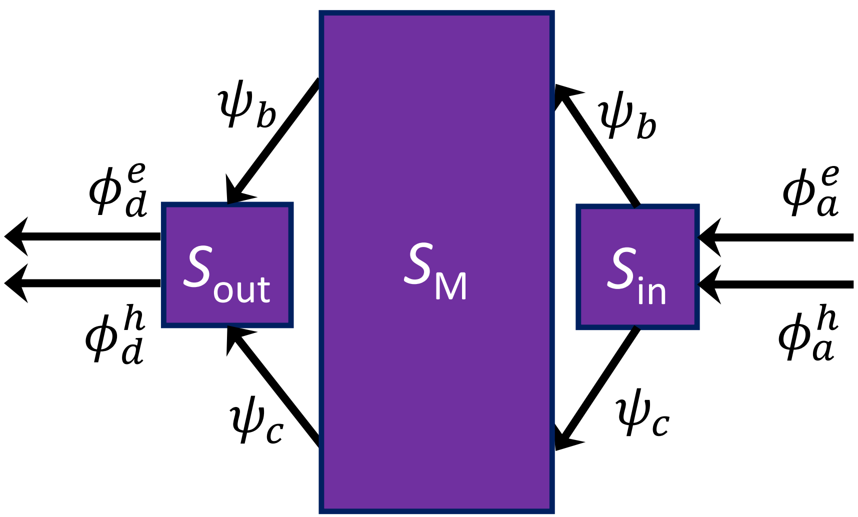

The full scattering matrix S of the Mach-Zehnder interferometer in Fig. 1 is given by the matrix product

$$S \equiv \begin{pmatrix} S_{ee} & S_{eh} \\ S_{he} & S_{hh}\end{pmatrix} = S_{\text{out}}\begin{pmatrix} e^{i\beta_b} & 0 \\ 0 & e^{i\beta_c}\end{pmatrix}S_{\text{in}}, \qquad (9)$$

where β_b and β_c are the phase shifts accumulated by the Majorana modes along edge b and c, respectively. The relative phase

$$\beta_b - \beta_c = \varepsilon\delta L/\hbar v_m + \pi + n_v\pi \qquad (10)$$

MQT in action: $\frac{dI}{dV}$ of topological system from S-matrix

- **S_M-matrix**

$$\begin{pmatrix}\psi_b\\ \psi_c\end{pmatrix}_{\text{out}} = \begin{pmatrix} e^{i\beta_b} & 0 \\ 0 & e^{i\beta_c}\end{pmatrix}\begin{pmatrix}\psi_b\\ \psi_c\end{pmatrix}_{\text{in}}$$

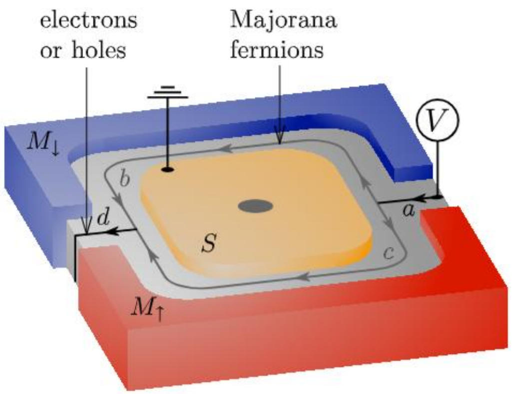

→ Just picking up phases with scattering. But we know

$$\beta_b - \beta_c = kL + \pi + n_v\pi = \frac{EL}{\hbar v_F} + \pi + n_v\pi$$

- **S-matrix**

$$S = \frac{1}{2}\begin{pmatrix} e^{i(\alpha+\alpha')}\left(e^{i\beta_b} - e^{i\beta_c}\right) & e^{-i(\alpha-\alpha')}\left(e^{i\beta_b} + e^{i\beta_c}\right) \\ e^{i(\alpha-\alpha')}\left(e^{i\beta_b} + e^{i\beta_c}\right) & e^{-i(\alpha+\alpha')}\left(e^{i\beta_b} - e^{i\beta_c}\right)\end{pmatrix}$$

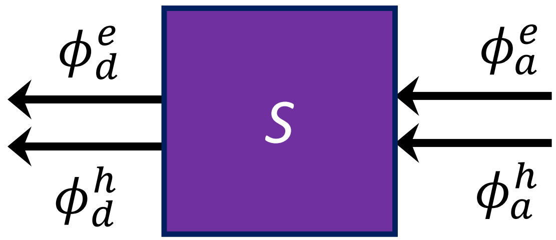

$$\begin{pmatrix}\phi_d^e\\ \phi_d^h\end{pmatrix} = S\begin{pmatrix}\phi_a^e\\ \phi_a^h\end{pmatrix}, S = \begin{pmatrix} S_{ee} & S_{eh} \\ S_{he} & S_{hh}\end{pmatrix}$$

The full scattering matrix S of the Mach-Zehnder interferometer in Fig. 1 is given by the matrix product

$$S \equiv \begin{pmatrix} S_{ee} & S_{eh} \\ S_{he} & S_{hh}\end{pmatrix} = S_{\text{out}}\begin{pmatrix} e^{i\beta_b} & 0 \\ 0 & e^{i\beta_c}\end{pmatrix} S_{\text{in}}, \tag{9}$$

where β_b and β_c are the phase shifts accumulated by the Majorana modes along edge b and c, respectively. The relative phase

$$\beta_b - \beta_c = \varepsilon\delta L/\hbar v_m + \pi + n_v\pi \tag{10}$$

MQT in action: $\frac{dI}{dV}$ of topological system from S-matrix

- **Quantum Transport using Landauer-Büttiker**

Negligible energy dependence of $T(E)$

$$I = I(V) = \frac{e}{h}\int_{\mu_R}^{\mu_L} T(E)dE = \frac{e^2}{h}TV$$

→ Charge transmission into Superconductor

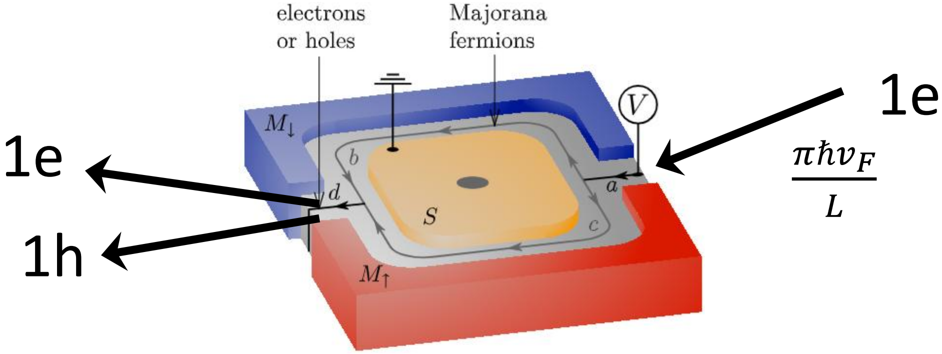

$$T = 1 - |S_{ee}|^2 + |S_{he}|^2 = 1 + |S_{he}|^2 - 1 + |S_{he}|^2 = 2|S_{he}|^2$$

from unitarity, $|S_{ee}|^2 + |S_{he}|^2 = 1$

$$G(0) = \frac{2e^2}{h}\sin^2\left(\frac{n_v\pi}{2}\right)$$

Finally, $\frac{dI}{dV} = \frac{2e^2}{h}|S_{he}|^2 = \frac{2e^2}{h}\sin^2\left(\frac{n_v\pi}{2} + \frac{eVL}{2\hbar v_F}\right)$

Electrons are incident at $E = eV$

MQT in action: $\frac{dI}{dV}$ of topological system from S-matrix

- **Physical pictures**

Electrically Detected Interferometry of Majorana Fermions in a TI
PRL **102**, 216404 (2009)

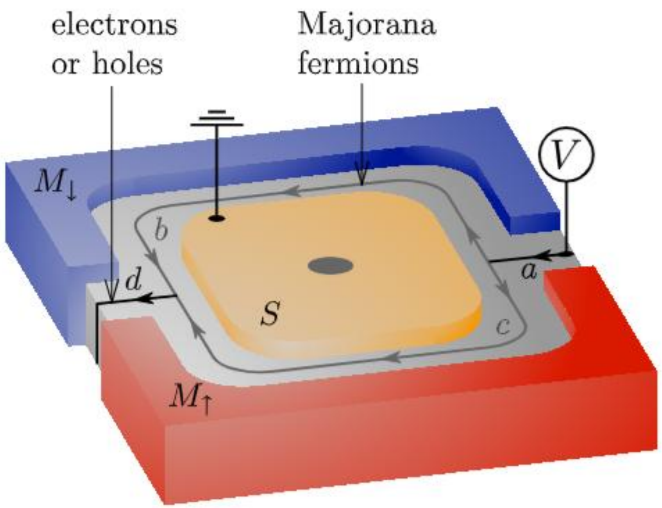

$$c_a^\dagger \to \gamma_b + i\gamma_c,$$

$$c_a \to \gamma_b - i\gamma_c.$$

Majorana Fermion Induced Resonant Andreev Reflection
PRL **103**, 237001 (2009)

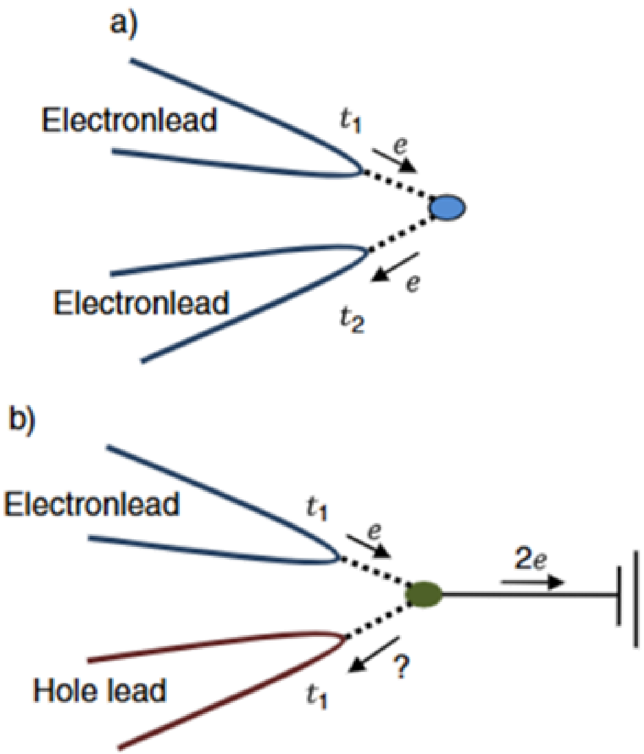

What left beyond today's lecture

- **More about Landauer-Büttiker formalism**

→ MQT is quantal: DC current = $\langle \hat{I} \rangle$, i.e., long-time average of current

→ Current shot noise is also available [M. Büttiker, *PRB* **46**, 12485 (1992)]

→ Periodically driven quantum pumps can be dealt [M. Büttiker, (1990)]

- **Beyond Landauer-Büttiker formalism: other methods for MQT**

Formalisms	Advantages	Disadvantages
Landauer-Büttiker	Intuitive & quick calculations. Finite voltage bias & temperature	Cannot deal with many-body physics
Kubo's linear response theory	Relatively easy & quick, while allowing many-body physics	Only allows physics around equilibrium states
Master equation	Allowing many-body physics & Nonequilibrium bias & finite temp.	Particularly useful at tunneling regime
Keldysh formalism	All the above	Not so easy for everyone